Molecular Biology of the Cell
Vol. 17, 4300–4317, October 2006

A Single Common Portal for Clathrin-mediated Endocytosis of Distinct Cargo Governed by Cargo-selective Adaptors[D] [V]

Peter A. Keyel,* Sanjay K. Mishra,* Robyn Roth,† John E. Heuser,† Simon C. Watkins,* and Linton M. Traub*

*Department of Cell Biology and Physiology, University of Pittsburgh School of Medicine, Pittsburgh, PA 15261; and †Department of Cell Biology and Physiology, Washington University School of Medicine, St. Louis, MO 63110

Submitted May 16, 2006; Revised July 18, 2006; Accepted July 19, 2006
Monitoring Editor: Sandra Schmid

Sorting of transmembrane cargo into clathrin-coated vesicles requires endocytic adaptors, yet RNA interference (RNAi)-mediated gene silencing of the AP-2 adaptor complex only disrupts internalization of a subset of clathrin-dependent cargo. This suggests alternate clathrin-associated sorting proteins participate in cargo capture at the cell surface, and a provocative recent proposal is that discrete endocytic cargo are sorted into compositionally and functionally distinct clathrin coats. We show here that the FXNPXY-type internalization signal within cytosolic domain of the LDL receptor is recognized redundantly by two phosphotyrosine-binding domain proteins, Dab2 and ARH; diminishing both proteins by RNAi leads to conspicuous LDL receptor accumulation at the cell surface. AP-2–dependent uptake of transferrin ensues relatively normally in the absence of Dab2 and ARH, clearly revealing delegation of sorting operations at the bud site. AP-2, Dab2, ARH, transferrin, and LDL receptors are all present within the vast majority of clathrin structures at the surface, challenging the general existence of specialized clathrin coats for segregated internalization of constitutively internalized cargo. However, Dab2 expression is exceptionally low in hepatocytes, likely accounting for the pathological hypercholesterolemia that accompanies ARH loss.

INTRODUCTION

When the clathrin coat was first discovered in mosquito oocytes (Roth and Porter, 1964), it was astutely speculated that the "bristle" coat provided cargo-selective properties that govern the process of yolk internalization. Mosquito yolk precursor receptors, the vitellogenin and lipophorin receptors, are members of the low-density lipoprotein (LDL) receptor superfamily. The first endocytic sorting signal was identified in this superfamily, when it was discovered that the ^{802}FDNPVY sequence within the carboxy-terminal cytosolic domain of human LDL receptor promotes rapid clathrin-mediated uptake of LDL (Davis *et al.*, 1986; Chen *et al.*, 1990). Other internalization signals have subsequently been identified, including the widespread YXXØ motif, found in transferrin and mannose 6-phosphate receptors, the [DE]XXXL[LI]-type dileucine motif, and reversible poly/multiubiquitination (Bonifacino and Traub, 2003).

To link these sorting signals to an assembling clathrin lattice, adaptor proteins are required because clathrin triskelia, the protomers of the characteristic polyhedral coat, contain no direct membrane-binding information. The first endocytic adaptor characterized was AP-2, a multifunctional heterotetramer comprised of a core of small σ2, medium μ2, and large α and β2 subunits. An independently folded appendage projects off each large subunit, connected to the core by a flexible polypeptide hinge (Owen *et al.*, 2004). The β2 subunit hinge and appendage bind physically to triskelia, allowing AP-2 to couple clathrin to the membrane, because the adaptor core binds phosphatidylinositol 4,5-bisphosphate (PtdIns(4,5)P_2) directly, and also interacts with YXXØ and [DE]XXXL[LI] motifs (Ohno *et al.*, 1995; Owen *et al.*, 2004; Höning *et al.*, 2005). Accordingly, AP-2 has a well-accepted role as the major cargo-selective component for endocytic coated vesicles. Nevertheless, distinct internalization signals neither saturate internalization at the same surface density nor compete directly with one another (Marks *et al.*, 1996; Santini *et al.*, 1998; Warren *et al.*, 1998), which is not expected if AP-2 performs all cargo-selective steps, and AP-2 does not readily bind to alternative internalization signals, including polyubiquitin and the FXNPXY sequence. Moreover, when small interfering RNA (siRNA) is used to ablate AP-2, transferrin uptake halts but cargo utilizing alternative endocytic signals, such as the LDL receptor, still internalize efficiently (Hinrichsen *et al.*, 2003; Motley *et al.*, 2003).

Endocytic clathrin coats must therefore contain alternative sorting adaptors. These clathrin-associated sorting proteins (CLASPs) should synchronously bind clathrin, the plasma membrane, cargo, and other lattice assembly proteins, such as AP-2 (Traub, 2003). Disabled-2 (Dab2) and the autosomal recessive hypercholesterolemia (ARH) protein are potential FXNPXY-signal–sorting CLASPs; both contain an amino-terminal phosphotyrosine-binding (PTB) domain that simultaneously interacts with nonphosphorylated FXNPXY motifs

This article was published online ahead of print in *MBC in Press* (http://www.molbiolcell.org/cgi/doi/10.1091/mbc.E06–05–0421) on July 26, 2006.

[D] [V] The online version of this article contains supplemental material at *MBC Online* (http://www.molbiolcell.org).

Address correspondence to: Linton M. Traub (traub@pitt.edu).

and PtdIns(4,5)P_2, along with an unstructured carboxy-terminal segment that contains tandemly arrayed clathrin- and AP-2–binding information (Morris and Cooper, 2001; He *et al.*, 2002; Mishra *et al.*, 2002a, 2002b; Yun *et al.*, 2003). Huge overexpression of a tandem Dab2 PTB domain construct selectively disrupts internalization of LDL receptor (Mishra *et al.*, 2002a) and the type-2 apolipoprotein E receptor (Cuitino *et al.*, 2005). However, this does not unambiguously prove the involvement of Dab2 in clathrin-mediated endocytosis; rather it shows a binary interaction between the PTB domain and the FXNPXY sorting signal. That Dab2-nullizygous mice exhibit a (mild) proteinuria, indicative of megalin (a hepatic scavenger receptor of the LDL receptor superfamily) dysfunction in the renal proximal tubule, supports a role for Dab2 in endocytosis. There are two major splice isoforms of Dab2, so-called p96 (full length) and p67, with the central AP-2 and clathrin binding region spliced out (Xu *et al.*, 1995). The poor ability of the p67 isoform to promote megalin-dependent transferrin uptake in developing embryos (Maurer and Cooper, 2005) also argues for Dab2 coupling cargo selection to clathrin coat assembly. Yet, conditionally-null Dab2$^{-/-}$ mice are surprisingly viable and fertile (Morris *et al.*, 2002). Conversely, targeted ARH gene disruption in mice, just as in ARH patients (Zuliani *et al.*, 1999; Garcia *et al.*, 2001; Arca *et al.*, 2002; Naoumova *et al.*, 2004), leads to elevated circulating LDL and LDL internalization defects in the liver (Jones *et al.*, 2003), but there is no evidence of proteinuria. These experiments hint at possible functional overlap between Dab2 and ARH activity in decoding FXNPXY sorting signals, but also uncover a seemingly complex interrelationship of the two proteins in vivo.

In this study, we show that Dab2 and ARH sort the LDL receptor in a functionally redundant manner; knocking down both proteins with siRNA causes extensive accumulation of LDL receptors at the cell surface. Assigning the CLASPs responsible for FXNPXY signal recognition is significant because LDL receptor superfamily members regulate numerous cellular processes; for instance, megalin appears to participate in steroid hormone action by promoting internalization of sex hormone–binding globulin complexes (Hammes *et al.*, 2005). In *Drosophila*, where the FXNPXY signal is conserved, lipoproteins play an important role transporting lipid-linked morphogens, such as Wingless and Hedgehog, and contribute to establishment of appropriate morphogen gradients during development (Panakova *et al.*, 2005), and this process might be conserved in chordates. In addition, clear appreciation of how Dab2 and ARH orchestrate FXNPXY sorting allows assessment of whether these CLASPs and cognate cargo are confined to functionally discrete subsets of clathrin structures at the plasma membrane. Despite recent propositions (Cao *et al.*, 1998; Tosoni *et al.*, 2005; Lakadamyali *et al.*, 2006), we do not find evidence of major compositional heterogeneity within clathrin coats at the surface of nonpolarized cells, questioning the general existence of specialized vesicles dedicated to internalization of select subsets of cargo.

MATERIALS AND METHODS

DNA Constructs and siRNA Duplexes

YFP-Dab2 was generated by first cloning EYFP into pECFP-N1 at the NheI and BglII sites, followed by replacing the in-frame CFP with full-length murine Dab2, inserted between the SalI and NotI sites. The plasmid was made RNA interference (RNAi)-resistant by introducing silent mutations (S249, L250, and R251) using QuikChange mutagenesis (Stratagene, La Jolla, CA). The GFP-epsin was created by cloning rat epsin 1 into pEGFP-C1 between the XhoI and KpnI sites, and the ARH-GFP was previously described (Mishra *et al.*, 2005). Appropriate mutations were introduced into either YFP-Dab2 or ARH-GFP using QuikChange mutagenesis with the required primers, the sequences of which are available on request. The siRNA oligonucleotides used, which target base pairs 1384–1402 of the AP-2 β2-subunit, base pairs 472–490 of dynamin 2, base pairs 1325–1343 of epsin 1, and base pairs 3313–3331 of the clathrin heavy chain (HC) nucleotide sequence, have been described (Hinrichsen *et al.*, 2003; Huang *et al.*, 2004). The Dab2 siRNA selected targets base pairs 745–763 of the Dab2 nucleotide sequence (UUCUUUAAGAGAAAAUCCA), the ARH siRNA targets base pairs 633–651 of the ARH nucleotide sequence (CCUGCUGGACUUAGAGGAG; Qiagen, Valencia, CA or Dharmacon, Lafayette, CO), and the β1 siRNA oligo targets base pairs 1529–1547 of the human β1 subunit nucleotide sequence (CCACUCAGGACUCAGAUAA; Invitrogen, Carlsbad, CA or Dharmacon). The ARH-specific siGENOME SMARTpool (M-013025–00) was also obtained from Dharmacon, as was the AP-2 α-subunit siRNA oligo that is essentially that previously described (Hinrichsen *et al.*, 2003) directed against base pairs 1052–1070 of the α subunit, although the final base pair of this sequence was omitted, yielding the sequence GCAUGUGCACGCUGGCCA. All siRNA oligos were synthesized with dTdT overhangs and directed against human sequences, unless otherwise noted.

Antibodies

The monoclonal antibodies (mAbs) against the clathrin HC TD.1 (Nathke *et al.*, 1992) and X22 (Brodsky, 1985); the anti-AP-1/2 β1/β2-subunit mAb 100/1 (Ahle *et al.*, 1988) and affinity-purified GD/1 antibodies (Traub *et al.*, 1995); the anti-AP-1 μ1-subunit antibody RY/1 (Traub *et al.*, 1996); the AP-2 α-subunit mAb AP.6 (Chin *et al.*, 1989), and affinity-purified anti-epsin 1 polyclonal (Drake *et al.*, 2000) have been described. Affinity-purified anti-eps15 polyclonal and anti-clathrin light chain polyclonal R461 were generous gifts from Ernst Ungewickell (Medizinische Hochschule Hannover, Hannover, Germany) and rabbit anti-AP-2 μ2-subunit serum was kindly provided by Juan Bonifacino (NIH, Bethesda, MD). Affinity-purified anti-LRP1 antibodies were kindly provided by Guojun Bu (Washington University School of Medicine, St. Louis, MO), the rat-isoform specific anti-LDL receptor polyclonal antibody was a kind gift from Gene Ness (University of South Florida, Tampa, FL), and the anti-α-mannosidase II antiserum was kindly provided by Kelley Moremen (University of Georgia, Athens, GA). A second mAb (clone 8) against the AP-2 α-subunit was purchased from BD Transduction Laboratories (San Jose, CA), and the anti-CD71/transferrin receptor mAb RVS-10 was from Chemicon (Temecula, CA). A goat anti-Dab2 polyclonal antibody was purchased from Santa Cruz Biotechnology (Santa Cruz, CA). The hybridoma secreting the anti-LDL receptor mAb IgG-C7 was obtained from the ATCC (Manassas, VA). The rodent-specific anti-asialoglycoprotein receptor mAb 8D7 was from HyCult Biotechnologies (Uden, The Netherlands). The anti-tubulin mAb E7 was purchased from the Developmental Studies Hybridoma Bank (Iowa City, IA). The affinity-purified ARH antibody (Mishra *et al.*, 2002b) was further cross-adsorbed with fixed and permeabilized ARH$^{-/-}$ fibroblasts, followed by removal of Hsc70 cross-reactivity by incubation with GST-DnaK bound to glutathione-Sepharose. The affinity-purified Dab2 (Mishra *et al.*, 2002a) antibody was similarly cross-adsorbed with immobilized GST-DnaK. Goat anti-mouse or anti-rabbit secondary antibodies conjugated to either AlexaFluor488 or AlexaFluor568 were purchased from Invitrogen, whereas goat anti-mouse or anti-rabbit antibodies conjugated to Cy5, HRP-conjugated donkey anti-mouse and anti-rabbit secondary antibodies, and colloidal gold-conjugated goat anti-rabbit secondary antibodies were purchased from Jackson ImmunoResearch (West Grove, PA). HRP-conjugated donkey anti-goat secondary antibody was from Santa Cruz.

Cell Culture, Transfections, RNAi, and Rescue Experiments

All cell lines were cultured at 37°C in a humidified atmosphere containing 5% CO_2. MCF-7 and MDA-MB-231 cells were grown in RPMI supplemented with 10% fetal calf serum (FCS; HyClone, Logan, UT) and 2 mM L-glutamine (Invitrogen), whereas primary control (GM01386) and ARH$^{-/-}$ (GM06697) fibroblasts and BS-C-1 cells were cultured in EMEM supplemented with 10% FCS, 2 mM L-glutamine and 1× nonessential amino acids (Mediatech, Herndon, VA). HeLa SS6 and HepG2 cells were cultured in DMEM supplemented with 10% FCS and 2 mM L-glutamine. BS-C-1 cells stably transfected with either the σ2-GFP or clathrin LCa-GFP were a generous gift from Tomas Kirchhausen (Harvard Medical School, Boston, MA) and cultured in DMEM supplemented with 10% FCS, 2 mM L-glutamine and 0.4 mg/ml G418 (Sigma, St. Louis, MO). For HeLa SS6 cell RNAi, the cells were passaged to yield 50–70% confluence in 24-well plates on the day of transfection. Transfections were performed with Transit-TKO reagent (Mirus Bio, Madison, WI) according to manufacturer's protocol using 100 nM of each siRNA. The culture media was replaced with fresh medium the following day, and cells were prepared for analysis 48–50 h after transfection with siRNA duplexes. For rescue experiments, 100 ng of rescue plasmid DNA was included along with the siRNA oligos at the time of transfection, and did not block RNAi-mediated knockdown of the proteins. Transfection of primary fibroblasts was performed by electroporating 2×10^6 cells using a Nucleofector II (Amaxa, Gaithersburg, MD), primary fibroblast electroporation solution (Amaxa), and 1 μM siRNA oligo according to the manufacturer's protocol with program U-023. Cells were passaged the following day and harvested ~72 h after

electroporation. Plasmid transfections were performed as previously described (Keyel *et al.*, 2004).

Immunofluorescence

Cells were prepared for immunofluorescence essentially as previously described (Mishra *et al.*, 2005). For experiments involving LDL receptors, the cells were grown in DMEM (for HeLa and BS-C-1 cells) or EMEM (for fibroblasts) supplemented with 10% lipoprotein-deficient serum (LPDS, Cocalico Biologicals, Reamstown, PA), 2 mM L-glutamine for 24–48 h before to up-regulate LDL receptors, whereas for experiments involving transferrin, cells were transferred to DMEM supplemented with 25 mM HEPES, pH 7.2, 0.5% BSA (starvation medium) for 1 h before experiments. To measure surface levels of receptors, cells were incubated with either the anti-LDL receptor mAb IgG-C7, anti-transferrin receptor mAb RVS-10, 4 μg/ml DiI-LDL (Biomedical Technologies, Stoughton, MA), 25 μg/ml transferrin conjugated to AlexaFluor488 (Tfn488; Invitrogen), or 50 μg/ml transferrin conjugated to AlexaFluor633 (Tfn633; Invitrogen) in starvation medium for 1 h on ice at 4°C, fixed, and processed for immunofluorescence. To measure the LDL and transferrin receptor internalization for RNAi and rescue experiments, after 1 h in starvation medium, cells were incubated in the continuous presence of either 4 μg/ml DiI-LDL alone, 4 μg/ml DiI-LDL with 50 μg/ml Tfn633, or 25 μg/ml Tfn conjugated to AlexaFluor568 (Tfn568) with mAb IgG-C7 for 15 min at 37°C before fixation and processing for immunofluorescence. To measure LDL receptor colocalization simultaneously with Dab2 and ARH, HeLa cells were transfected with YFP-Dab2, cultured in DMEM containing 10% LPDS and 2 mM L-glutamine for ~24 h, incubated with mAb IgG-C7 for 1 or 5 min at 37°C, permeabilized on ice with 0.3% saponin, 25 mM HEPES-KOH, pH 7.2, 125 mM potassium acetate, 5 mM magnesium acetate, 2 mM EDTA, 2 mM EGTA for 1 min, fixed, and processed for immunofluorescence.

Fluorescence Microscopy

Images were acquired either on an Olympus Fluoview 500 or Olympus 1000 confocal microscope (Melville, NY) by sequentially scanning by line with an argon laser for 488-nm excitation, and two helium-neon lasers for 543- and 633-nm excitation through a PlanApomat 60 × 1.40 NA objective with a 488/543/633 dichroic. Emitted light was separated with beam splitters SDM560 and SDM640 and passed through either bandpass filters BA505–525 (green), BA560–600 (red) and longpass filter BA660IF (cy5) on the Fluoview 500 or diffraction gratings that pass 500–530-nm (green) or 555–625-nm (red) light or a BA650IF filter (cy5) on the Fluoview 1000 before detection. Linescan analysis of Dab2 and surface LDL receptor fluorescence along arbitrary 76-pixel lines using the average integrated intensity of three perpendicular pixels for each point along the line was measured in Metamorph (Molecular Devices, Downingtown, PA). Quantitation of the colocalization between various clathrin coat components was performed as described (Hawryluk *et al.*, 2006). Quantitation of the rescue of the RNAi phenotype was measured by counting the number of transfected cells showing either normal, impaired, or no LDL receptor internalization and displaying each as a percentage of the total cells counted. A small portion of plasmid-transfected cells displayed an overexpression phenotype (Mishra *et al.*, 2005); these were excluded from the analysis. For fluorescence recovery after photobleaching (FRAP) experiments, HeLa cells grown on chambered glass coverslips (Nalge Nunc International, Rochester, NY) were transfected with either YFP-Dab2 or ARH-GFP and imaged every 5.2 s with the argon 488-nm laser line on the Fluoview 1000. A 405-nm laser diode was used at maximum intensity for 5 s to bleach YFP-Dab2 or ARH-GFP fluorescence during the acquisition. The intensity of each bleached region was measured using Metamorph, corrected for background, and each plane normalized to the intensity of an unbleached cell to account for any fluctuations in focus or intensity and then normalized to the average intensity of the frames before the bleach. To follow LDL and transferrin internalization in the context of the knockdown, RNAi-treated, serum-starved HeLa cells were incubated with 25 μg/ml Tfn488 and 4 μg/ml DiI-LDL and imaged every 3–6 s. To visualize LDL internalization in real time, HeLa cells in chambered glass coverslips transfected with YFP-Dab2 were imaged every 3–4 s in starvation medium. During image acquisition, starvation medium containing DiI-LDL was added such that the final concentration of DiI-LDL was 4 μg/ml. Measurement of DiI-LDL and YFP-Dab2 intensity in Dab2 structures that accumulated LDL within 250 s of LDL addition was performed using Metamorph; 17 structures were measured and averaged. For all live-cell experiments, at least five separate cells were imaged, and experiments were repeated at least twice.

Electron Microscopy

Cells cultured in LPDS were surface labeled with 50 μg/ml LDL (Biomedical Technologies) or not, before preparing "unroofed" cell cortices for rapid-freeze deep-etch electron microscopy (EM) essentially as previously described (Heuser, 2000; Edeling *et al.*, 2006). Briefly, cells grown on small oriented, carbon-coated coverslips were disrupted by sonication directly in 2% paraformaldehyde, 0.025% glutaraldehyde in 30 mM HEPES-KOH, pH 7.3, 70 mM potassium chloride, 5 mM magnesium chloride, and 3 mM EGTA (KHMgE buffer). After washing, preparations were quenched with 50 mM ammonium chloride, 50 mM L-lysine in KHMgE and blocked with 1% BSA in KHMgE, followed by incubation with affinity-purified anti-Dab2 or anti-ARH antibodies and then 15-nm colloidal gold-conjugated anti-rabbit antibody. Finally, the membranes were fixed in 2% glutaraldehyde before freezing. For surface labeling, washed cells were fixed directly in 2% glutaraldehyde without sonication.

Tissue and Cell Preparation

Rat liver Golgi membranes (Tabas and Kornfeld, 1979) and plasma membrane sheets (Hubbard *et al.*, 1983) were prepared using published protocols. Freshly isolated rat hepatocyte and total rat liver nonhepatocyte cell fractions were kind gifts from William Bowen, Jr. For Western blots, cells were trypsinized, washed in PBS, lysed directly in boiling SDS-sample buffer, heated to 95°C for 5 min, sonicated to shear DNA, and centrifuged at 12,000 × g_{max} for 2 min to pellet insoluble material. Protein levels were standardized using a Coomassie blue–based filter paper binding assay (Minamide and Bamburg, 1990); 25 μg was loaded per lane. Rat liver samples were prepared by finely mincing the tissue with a razor blade at 0°C, homogenizing in a small volume 10 mM HEPES-KOH, pH 7.2, 0.3 M sucrose, and Complete protease inhibitor (Roche, Indianapolis, IN) with a Teflon homogenizer, and solubilizing directly in boiling SDS-sample buffer or in nonreducing SDS-sample buffer at 37°C. After incubation at either 95 or 37°C, respectively, for 5 min, the samples were sonicated and centrifuged at 12,000 × g_{max} for 2 min to pellet insoluble material.

Liposome-binding Assays

Sedimentation binding assays utilizing either multilamellar control liposomes composed of 40% phosphatidylcholine, 40% phosphatidylethanolamine, 10% phosphatidylserine, and 10% cholesterol or PtdIns(4,5)P_2-containing liposomes composed of 35% phosphatidylcholine, 35% phosphatidylethanolamine, 10% phosphatidylserine, 10% cholesterol, and 10% PtdIns(4,5)P_2 were performed as described previously (Mishra *et al.*, 2002a, 2002b).

Electrophoresis and Immunoblotting

Samples were resolved on polyacrylamide gels prepared with an altered acrylamide:bis-acrylamide (30:0.4) ratio stock solution. The decreased cross-linking generally improves resolution but also affects the relative mobility of several proteins, most noticeably epsin 1. After SDS-PAGE, proteins were either stained with Coomassie blue or transferred to nitrocellulose in ice-cold 15.6 mM Tris, 120 mM glycine. Blots were usually blocked overnight in 5% skim milk in 10 mM Tris-HCl, pH 7.8, 150 mM NaCl, 0.1% Tween 20, and then portions were incubated with primary antibodies as indicated in the individual figure legends. After incubation with HRP-conjugated anti-mouse or anti-rabbit IgG, immunoreactive bands were visualized with enhanced chemiluminescence. Alternatively, donkey anti-rabbit IgG was iodinated with ICl utilizing an established method (Breitfeld *et al.*, 1989) and used at 200,000 cpm/ml to detect the bands. Quantitation of the signal from blots was performed using a Phosphor-Imager (Bio-Rad, Hercules, CA).

RESULTS

Selective LDL Receptor Internalization by Dab2 and ARH

Cultured fibroblasts derived from ARH patients do not display major defects in LDL uptake, unlike LDL receptor-defective fibroblasts from individuals with familial hypercholesterolemia (Garcia *et al.*, 2001; Eden *et al.*, 2002). Because ARH$^{-/-}$ fibroblasts do express Dab2 (Mishra *et al.*, 2002b), the common domain/sequence signatures and functional analogy between ARH and Dab2 suggest that Dab2 might compensate for the absence of ARH in these cells. Indeed, Dab2 is positioned in small puncta scattered apparently randomly over the surface of ARH-null cells, most of which colocalize with both AP-2 and the LDL receptor (Figure 1, A and B). Transiently knocking down Dab2 levels by transfection with siRNA oligonucleotides (Figure 1C) strongly diminishes Dab2 staining, but the AP-2 distribution is unaltered (Figure 1D). In ARH$^{-/-}$ cells with depressed Dab2 levels, the LDL receptor diffuses over the cell surface and weak foci of clustered receptor, compared with adjacent non–gene-silenced cells, correspond mostly to clathrin-coated regions harboring residual Dab2 (Figure 1E). Fluorescence intensity analysis of these images shows clearly that in ARH$^{-/-}$ fibroblasts, peaks of LDL receptor labeling coincide precisely with a Dab2 signal but that there is negligible correspondence with the more diffuse LDL receptor after diminishing Dab2 protein levels (Supplementary Figure S1). By contrast, the transferrin receptor remains concentrated at bud sites

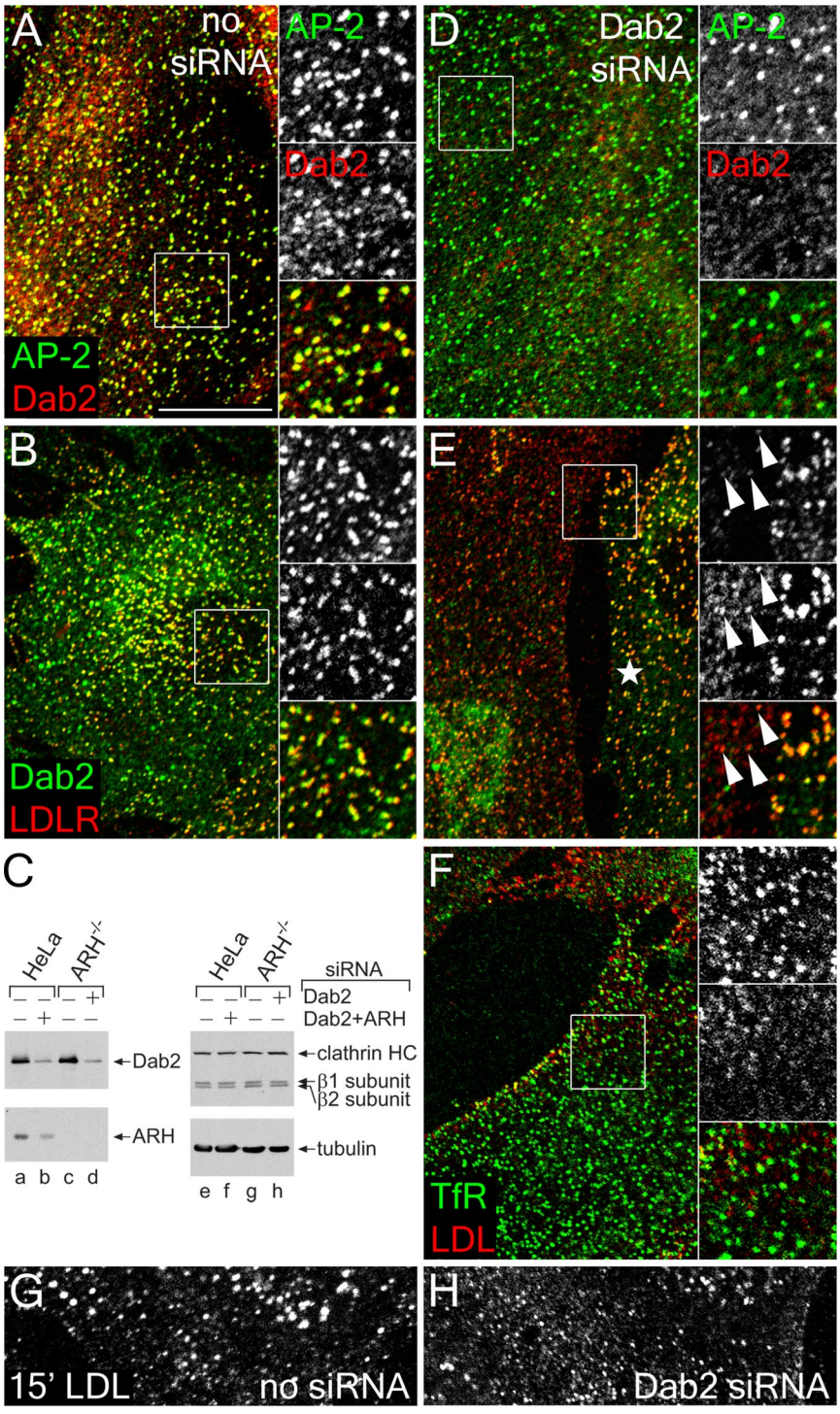

Figure 1. Dab2 activity in ARH-null fibroblasts. GM00697 ARH$^{-/-}$ fibroblasts nucleofected with mock (A, B, and G) or Dab2-specific siRNA duplexes (D–F and H) were fixed and stained with anti-AP-2 α subunit mAb AP.6 and/or affinity-purified anti-Dab2 antibodies, or, before fixation, were incubated on ice with anti-LDL receptor mAb IgG-C7 (LDLR), or anti-transferrin receptor (TfR) mAb RVS-10 and DiI-LDL on ice for 60 min. Representative single confocal optical sections are shown with color-separated AP-2 (green channel, top) and Dab2 (red channel, middle) and merged magnifications of each boxed region shown on the right. Alternatively, whole cell lysates from HeLa SS6 or ARH$^{-/-}$ fibroblast transfected with mock, Dab2+ARH, or Dab2 siRNA duplexes were prepared, resolved by SDS-PAGE, and transferred to nitrocellulose (C). Portions of the blots were probed with anti-Dab2 or ARH polyclonal antibodies, anti-clathrin heavy chain (HC) mAb TD.1 and anti-β1/β2 subunit mAb 100/1, or anti-tubulin mAb E7, and only the relevant region of each blot is shown. Mock (G) or Dab2 siRNA transfected (H) ARH$^{-/-}$ fibroblast cells were also incubated with DiI-LDL at 37°C for 15 min before fixation. In E, an untransfected cell is indicated with an asterisk, and residual Dab2-positive structures containing LDL receptor are shown with arrowheads. Scale bar, 10 μm.

irrespective of the intracellular Dab2 concentration (Figure 1F). Internalization of DiI-labeled LDL and subsequent concentration in perinuclear endosomes is also obviously slowed in ARH$^{-/-}$ cells with decreased Dab2 levels (Figure 1, G and H). Together, these results suggest that Dab2 actively clusters LDL receptors at clathrin bud sites in ARH nullizygous fibroblasts.

In HeLa cells, RNAi-mediated gene silencing of either Dab2 or ARH transcripts (Figure 2A) results in only mild impairment of LDL uptake. Compared with control cells, LDL receptors accumulate at the cell surface, although substantial LDL internalization is evident (Figure 2, C and D). Again, transferrin endocytosis proceeds normally in both control and RNAi-treated cells, and the intracellular transferrin colocalizes, in part, with internalized LDL. Yet, simultaneously knocking down both ARH and Dab2 with siRNA duplexes has a dramatic effect on LDL receptor trafficking (Figure 2E). LDL accumulates diffusely over the surface, but transferrin uptake continues relatively unimpeded. Anti-LDL receptor antibody binding shows a surface density increase of at least fivefold after Dab2+ARH RNAi. Time-

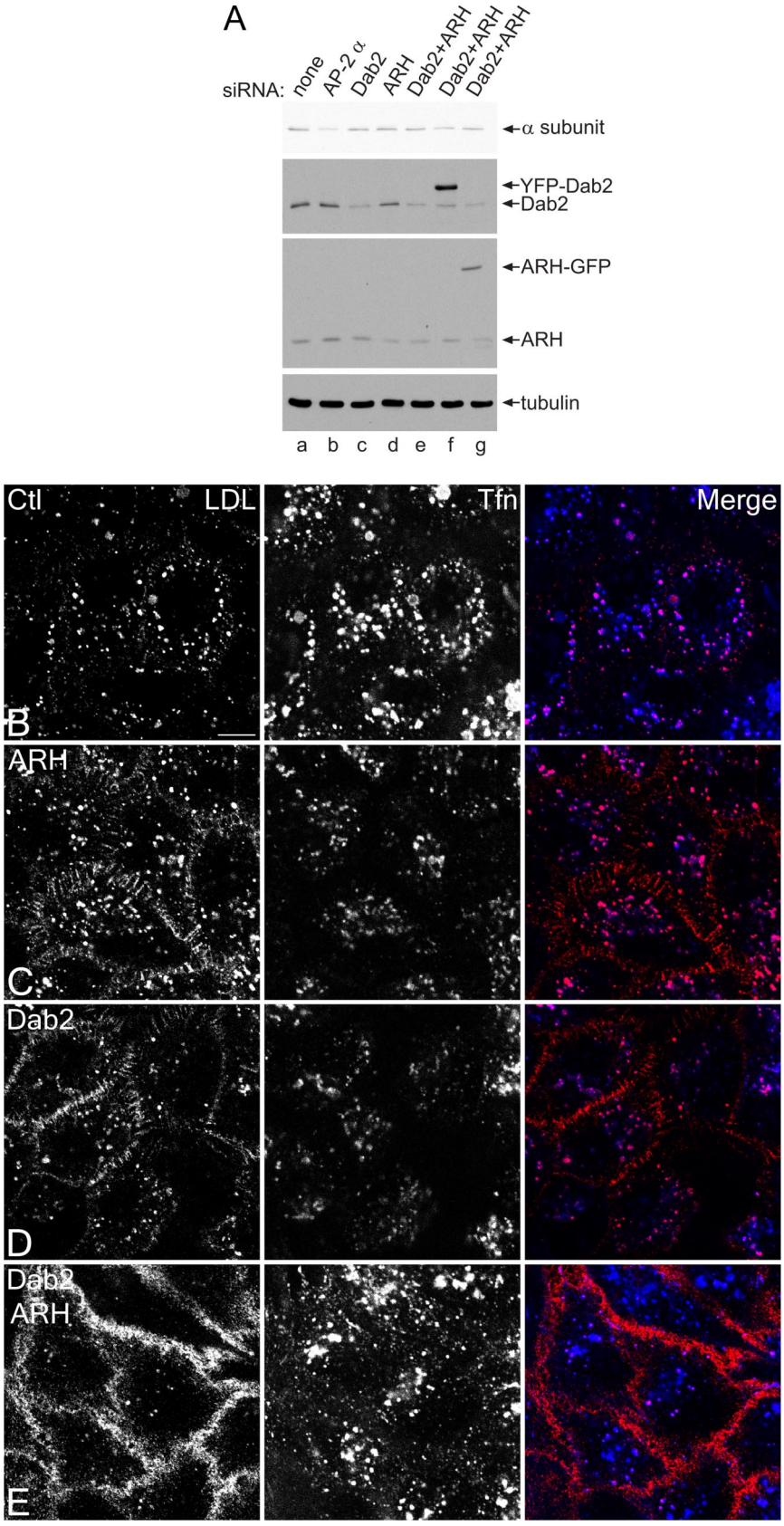

Figure 2. Cargo selective effect of Dab2 and ARH gene silencing. HeLa SS6 cells transiently transfected with mock (A, lane a, and B) or siRNA duplexes targeting the AP-2 α subunit (A, lane b), Dab2 (A, lane c, and D), ARH (A, lane d, and C), or Dab2+ARH alone (A, lane e, and E), or together with YFP-Dab2 (A, lane f) or ARH-GFP (A, lane g) were lysed, resolved by SDS-PAGE, and transferred to nitrocellulose. Portions of the blots were probed with anti-AP-2 α subunit mAb clone 8, anti-Dab2 or anti-ARH polyclonal antibodies, or anti-tubulin mAb E7 (A). Only the relevant portions of the blots are shown. Alternatively, transfected cells on coverslips were incubated together with 4 μg/ml DiI-LDL (left, red in merge) and 50 μg/ml Tfn633 (center, blue in merge) for 15 min at 37°C and fixed (B–E). Representative single confocal optical sections are shown. Note the pronounced surface accumulation of LDL, but not transferrin, in the Dab2+ARH knockdown and to a much lesser extent in the single knockdowns. Scale bar, 10 μm.

resolved imaging of cells incubated with fluorescent LDL and transferrin confirms the severe effect of the Dab2+ARH double knockdown. Although LDL and transferrin are efficiently internalized and some sorted into common endo-

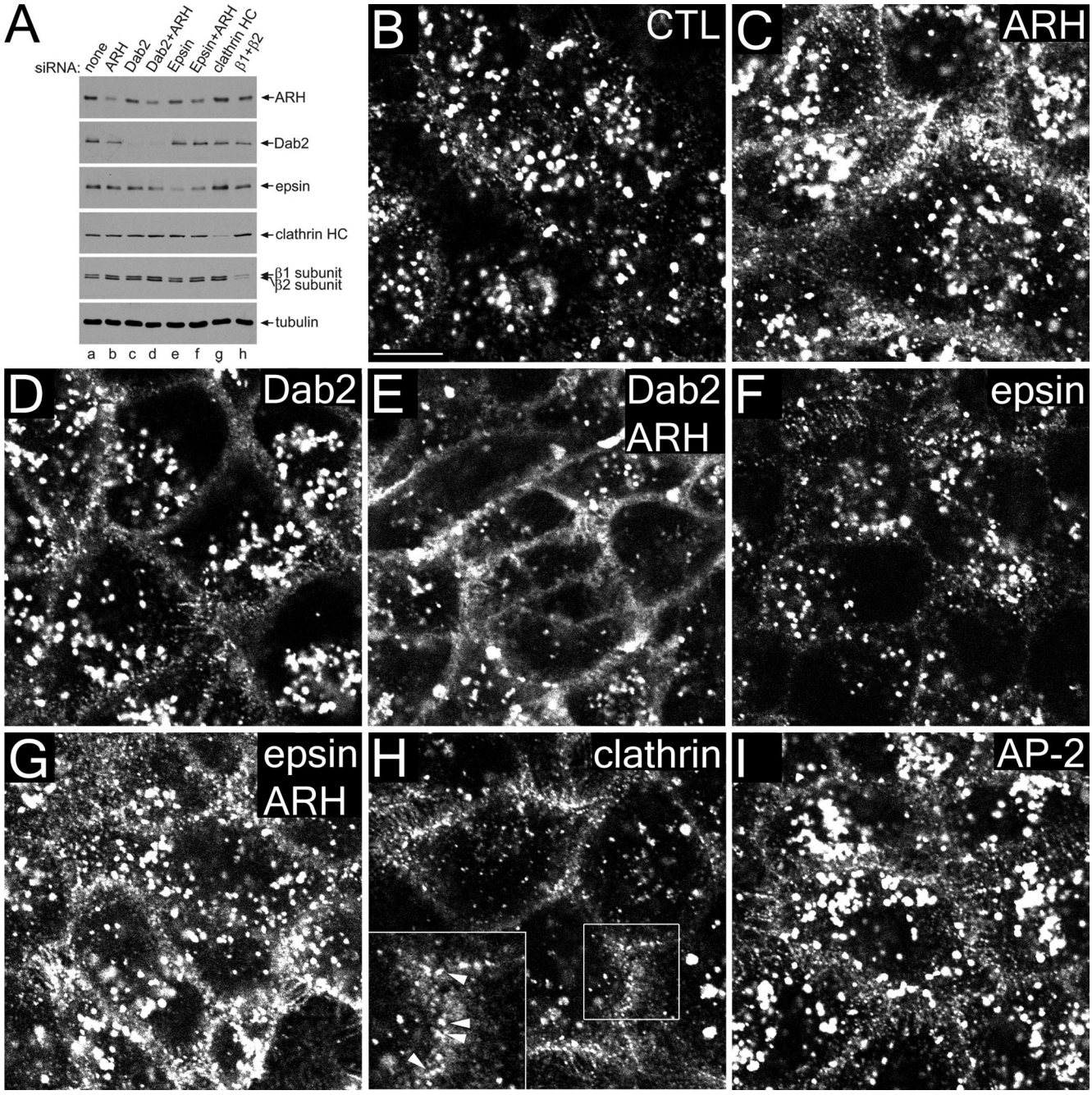

Figure 3. Dab2 and ARH are LDL-specific CLASPs. HeLa SS6 cells transiently transfected with mock (A, lane a, and B) or with specific siRNA duplexes directed against ARH (A, lane b, and C), Dab2 (A, lane c, and D), Dab2+ARH (A, lane d, and E), epsin 1 (A, lane e, and F), epsin1+ARH (A, lane f, and G), clathrin heavy chain (A, lane g, and H), or AP-1 β1 and AP-2 β2 subunits (A, lane h, and I) were lysed, resolved by SDS-PAGE, and transferred to nitrocellulose. Portions of the blots were probed with either affinity-purified anti-ARH, anti-Dab2, or anti-epsin 1, anti-β1/β2 subunit mAb 100/1 antibodies, anti-clathrin HC mAb TD.1, or anti-tubulin mAb E7. Alternatively, transfected cells on coverslips were incubated with 4 μg/ml DiI-LDL for 15 min at 37°C and fixed (B–I). Representative single confocal optical sections are shown with a magnification of the boxed region in H shown on the lower left. Note the dramatic surface accumulation and diminished internalization of LDL in clathrin or Dab2+ARH double knockdowns, but some surface LDL still appears clustered in puncta in the absence of clathrin (H inset, arrowheads). Scale bar, 10 μm.

somes in the mock-treated HeLa cells, the surface of the siRNA-treated cells is heavily labeled with LDL, also diffusing into filopodia despite normal transport of transferrin to the cell interior (Supplementary Movie 1). Strikingly, these results are the reciprocal of those obtained when AP-2 levels are reduced >75% by RNAi, where transferrin but not LDL accumulates at the cell surface (Hinrichsen *et al.*, 2003; Motley *et al.*, 2003; see also Figure 6, A and B).

Because Dab2 has multiple clathrin-binding sites like AP-2 (Mishra *et al.*, 2002a), it is possible that general clathrin lattice assembly is impaired in the Dab2+ARH double knockdowns and this, rather than sorting aberrations, is

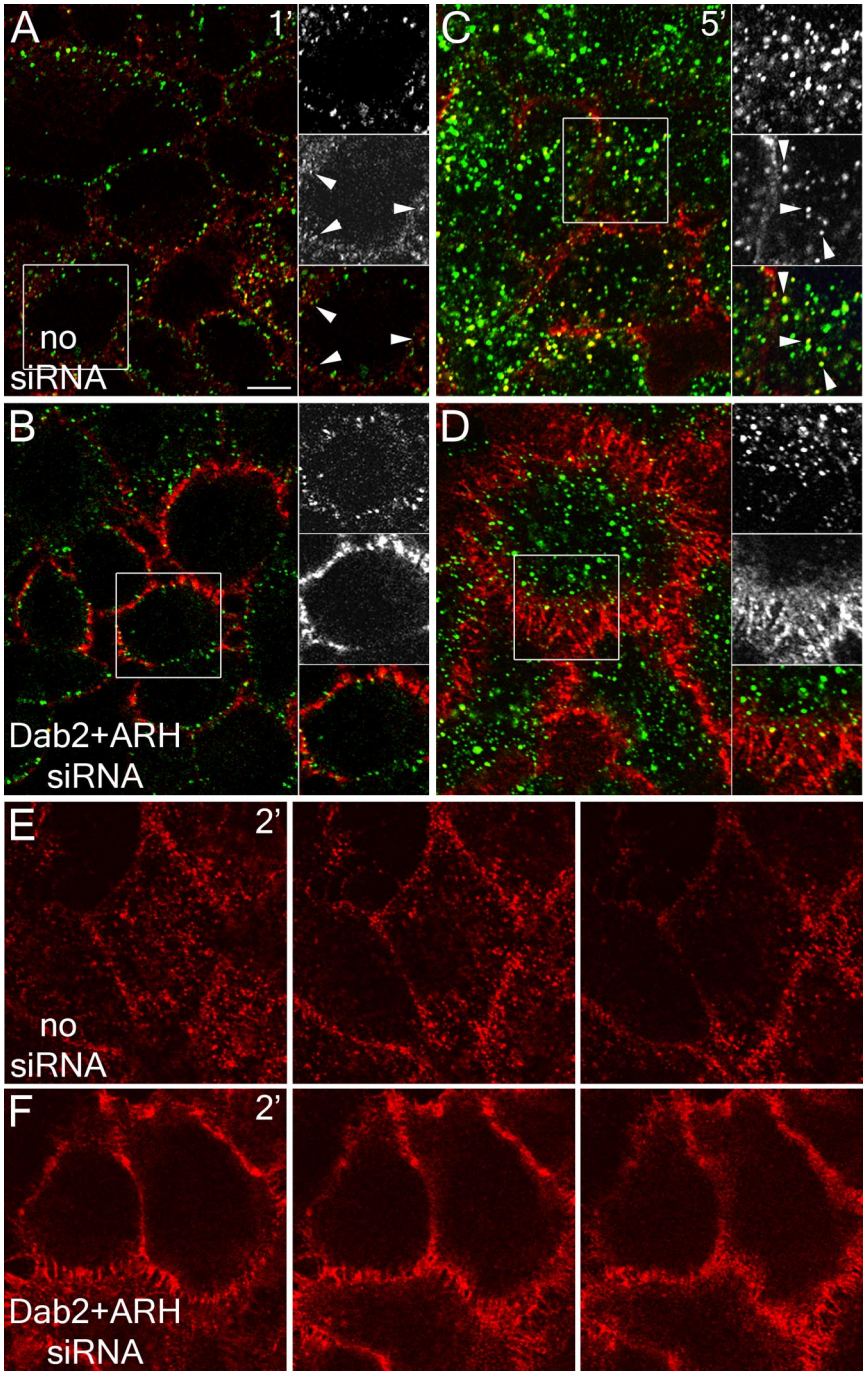

Figure 4. Slowed LDL uptake in Dab2- and ARH-depleted HeLa cells. (A–D) HeLa SS6 cells either mock transfected (A and C) or transfected with Dab2+ARH siRNA duplexes (B and D) were incubated at 37°C in the continuous presence of both 25 μg/ml Tfn488 (green) and 5 μg/ml DiI-LDL (red) either for 1 (A and B) or 5 min (C and D), rapidly washed on ice, and then fixed. The boxed regions are enlarged at the right of each image, with transferrin (green), LDL (red) and merged channels shown. Arrowheads mark punctate endosomal structures. Importantly, the DiI-LDL concentration used is considerably lower than the ~50 μg/ml required to saturate the surface LDL receptor in control cells (Brown and Goldstein, 1986) and, consequently, not all LDL receptors are occupied under these conditions. (E and F) HeLa SS6 cells either mock transfected (E) or transfected with Dab2+ARH siRNA duplexes (F) were incubated at 37°C with 5 μg/ml DiI-LDL for 2 min, washed on ice, and fixed. Representative sequential confocal optical sections are shown to illustrate the general delay in LDL internalization in the Dab2+ARH-depleted cells. Scale bar, 10 μm.

responsible for the surface LDL accumulation. However, RNAi of epsin 1, an abundant poly/multiubiquitin-selective CLASP with multiple clathrin-binding sites, does not produce a similar effect. Despite >80% decrease in epsin levels in siRNA-transfected HeLa cells (Figure 3A), LDL uptake is similar in control and epsin-depleted cells (Figure 3, B and F), and in ARH or epsin+ARH knocked-down cells (Figure 2, C and G). Still, tandem Dab2+ARH knockdown severely blocks LDL internalization, with characteristic accumulation of surface LDL (Figure 3E). Clathrin (and dynamin 2; unpublished data), but not AP-2, ablation likewise inhibits LDL internalization, though the LDL still accumulates in punctate structures on the surface, which, given the presence of LDL-selective CLASPs and the fact that adaptors/CLASPs retain appropriate intracellular positioning in the absence of clathrin (Hinrichsen *et al.*, 2006), is expected (Figure 3, H and I, arrowheads). In these experiments, the extent of ARH depletion is somewhat variable (compare Figures 2A, 3A, and 6A). Nevertheless, no substantial increase in the extent of ARH gene silencing is seen if a multiple siRNA-containing SMARTpool is used instead of the single duplex used for the majority of this study. In both cases, ~80% decrease in steady state ARH levels can be achieved (Supplementary Figure S2).

A clear kinetic lag in the uptake of DiI-LDL occurs in Dab2+ARH-silenced cells (Figure 4 and Supplementary Fig-

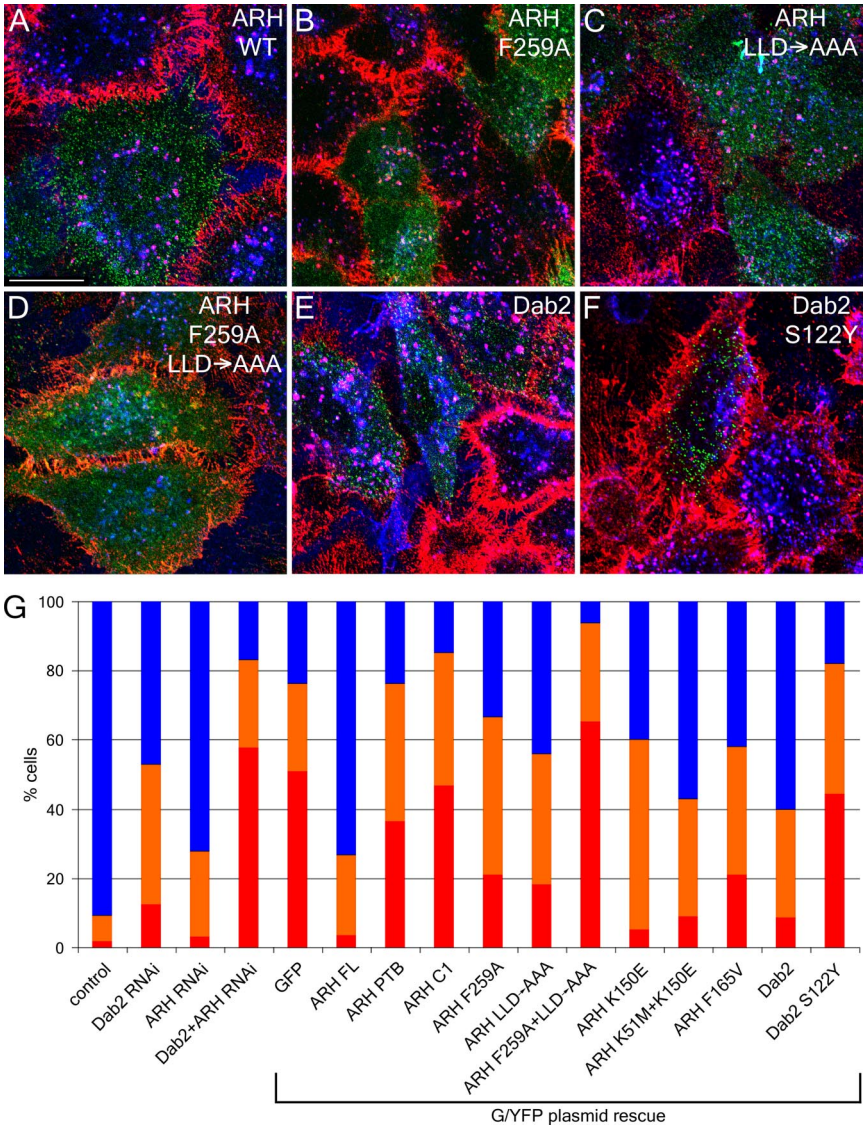

Figure 5. Cargo- and AP-2–binding domains of ARH and Dab2 are necessary for LDL sorting. HeLa SS6 cells transiently transfected with siRNAs targeting both ARH and Dab2 along with either wild-type ARH-GFP (A), or F259A (B), ^{212}LLD→AAA (C), F259A+^{212}LLD→AAA (D) ARH mutations, or wild-type YFP-Dab2 (E) or a S122Y Dab2 mutation (F), were grown in DMEM with LPDS overnight, incubated with 4 μg/ml DiI-LDL (red) and 50 μg/ml Tfn633 (blue) for 15 min at 37°C, and then fixed. Scale bar, 10 μm. (G) Quantitation of various ARH-GFP or YFP-Dab2 constructs rescuing LDL internalization. The percentage of cells showing normal (blue), impaired (approximating the level of LDL internalization seen in ARH or Dab2 single knockdowns; orange), or blocked LDL internalization (red) was determined for control (n = 1194 cells), Dab2 (n = 718), ARH (n = 686) or Dab2+ARH (n = 3455) siRNA-treated cells or for the Dab2+ARH siRNA background with rescue plasmids GFP (n = 412), ARH full-length (ARH FL, n = 231), ARH residues 1–179 (ARH PTB, n = 195), ARH residues 180–308 (ARHC1, n = 177), ARH F259A (n = 235), ARH LLD→AAA (n = 93), ARH F259A+LLD→AAA (n = 178), ARH K150E (n = 20), ARH K51M+K150M (n = 91), ARH F156V (n = 110), Dab2 (n = 183), or Dab2 S122Y (n = 45).

ure S3). Both transferrin and LDL populate common peripheral endosomes in control cells incubated for 5 min in the continuous presence of both ligands (Figure 4C and Supplementary Figure S3). Between 20 and 40 min marked concentration of LDL in juxtanuclear endosomes is apparent (Supplementary Figure S3B and C). A low level of LDL is present at the surface in the control cells between 1 and 5 min (Figure 4, A, C, and E, and Supplementary Figure S3, A and G), which is in accord with both the lower absolute rate of internalization and a less abundant rate-limiting component for LDL uptake compared with transferrin (Warren *et al.*, 1998). In the Dab2+ARH-depleted cells, already between 1 and 5 min, very prominent appearance of a circumferential band of LDL at the plasma membrane occurs and is still evident at 40 min (Supplementary Figure S3F). Although LDL endocytosis is slowed (compare Figure 4, F to E), the ligand is nonetheless still internalized and traffics to the transferrin-positive early endosome compartment, but not as efficiently as in mock-treated cells (Supplementary Figure S4G). This overall slowed internalization of LDL in the FXNPXY-selective CLASP-depleted cells is fully consistent with the about fivefold reduction in internalization index characteristic of LDL receptor FXNPXY mutants devoid of an operational sorting signal (Davis *et al.*, 1986, 1987; Chen *et al.*, 1990).

Importantly, efficient LDL uptake is restored upon transient expression of either an ARH-GFP or an siRNA-resistant YFP-Dab2 fusion protein in Dab2+ARH knockdown cells (Figure 5, A and E). This demonstrates that either of these proteins can individually restore LDL uptake and that the appended fluorescent tags do not significantly interfere with LDL endocytosis. We conclude that Dab2 and ARH appear to operate in a functionally redundant manner to drive the efficient internalization of the LDL receptor in nonpolarized cells and that the YXXØ (transferrin receptor) and FXNPXY (LDL receptor) sorting signals are decoded by distinct components of the clathrin coat.

Functional Modules within ARH and Dab2

Dab2 and ARH each contain cargo- (FXNPXY), PtdIns(4,5)P_2-, AP-2-, and clathrin-binding regions, which allow direct coupling of bound cargo to the clathrin coat machinery (Morris and Cooper, 2001; He *et al.*, 2002; Mishra *et al.*, 2002a, 2002b; Garuti *et al.*, 2005). If either the AP-2– or the clathrin-binding

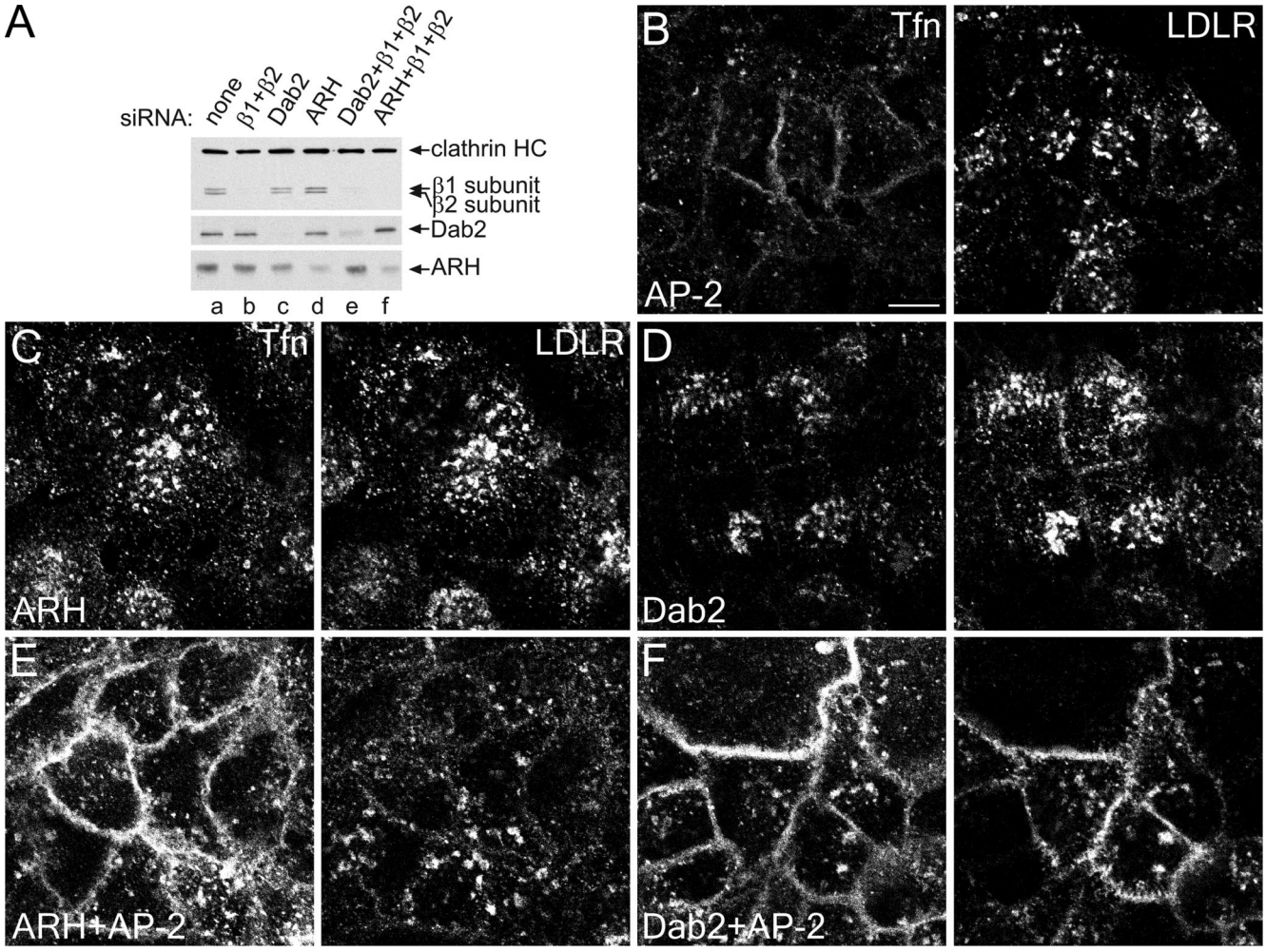

Figure 6. ARH requires AP-2 for LDL-sorting function. HeLa SS6 cells mock-transfected (A, lane a) or transfected with AP-2 ($\beta1+\beta2$ subunits; A, lane b, and B), Dab2 (A, lane c, and D), ARH (A, lane d, and C), or Dab2+$\beta1+\beta2$ (A, lane e, and F) or ARH+$\beta1+\beta2$ (A, lane f, and E) specific siRNA duplexes grown overnight in DMEM with 10% LPDS were lysed, resolved by SDS-PAGE and transferred to nitrocellulose. Portions of replicate blots were probed with anti-clathrin heavy-chain mAb TD.1, anti-$\beta1/\beta2$ subunit mAb 100/1, or polyclonal anti-Dab2 or anti-ARH antibodies (A). Alternatively, transfected cells on coverslips were incubated for 15 min at 37°C with 25 μg/ml Tfn568 (Tfn) and anti-LDL receptor mAb IgG-C7 (LDLR) before fixing (B–F). Representative single confocal optical sections are shown. Scale bar, 10 μm.

information within ARH-GFP is singly compromised by mutation of either F259A or ^{212}LLD→AAA, respectively, the expressed protein still promotes LDL internalization (Figure 5, B and C), though quantitation reveals that neither mutant rescues fully (Figure 5G; Garuti *et al.,* 2005). These results are reminiscent of data obtained when the analogous binding sequences for clathrin or AP-2 are singly altered in β-arrestin 2 (Laporte *et al.,* 2000; Kim and Benovic, 2002; Santini *et al.,* 2002). When both these binding sites are disrupted, the ARH-GFP becomes diffusely distributed in the cytoplasm and fails to rescue the Dab2+ARH knockdown phenotype (Figure 5D). S122Y, a PTB domain mutation affecting the FXNPXY binding surface of YFP-Dab2 (Stolt *et al.,* 2004), similarly prevents restoration of LDL internalization (Figure 5F), even with the expressed Dab2 still residing in puncta that colocalize with clathrin. By contrast, mutations to the phosphoinositide binding region (K51M and K150E) of the ARH PTB domain are still compatible with LDL internalization (Figure 5G), despite strongly interfering with ARH binding to PtdIns(4,5)P_2 in vitro (Supplementary Figure S4). This affirms that the lipid-binding surface of ARH is juxtaposed to, but functionally separate from, the FXNPXY contact site (Mishra *et al.,* 2002a, 2002b; Stolt *et al.,* 2004). Thus, Dab2 and ARH (when overexpressed) require engagement of both cargo and core coat components for proper LDL receptor sorting, whereas additional interactions with PtdIns(4,5)P_2 and clathrin likely increase the efficiency of the process.

ARH Requires AP-2 to Drive LDL Uptake

Despite the apparent functional redundancy of Dab2 and ARH, the two CLASPs clearly engage the AP-2 adaptor in molecularly distinct ways. Dab2 has several low-affinity (K_D ~50–150 μM), tandemly arrayed α appendage–binding motifs (Morris and Cooper, 2001; Mishra *et al.,* 2002a), whereas ARH has only a single, moderate affinity (K_D 1–2 μM) AP-2 interaction sequence with an absolute selectivity for the $\beta2$ appendage (He *et al.,* 2002; Mishra *et al.,* 2002b, 2005). β-arrestins have a related, α-helical $[DE]_nX_{1-2}FXX[FL]XXXR$ motif that binds the platform subdomain of the $\beta2$ appendage (Mishra *et al.,* 2005; Edeling *et al.,* 2006; Schmid *et al.,* 2006). Consequently, ARH might function similarly to β-arrestins, not participating directly in clathrin lattice assembly, but

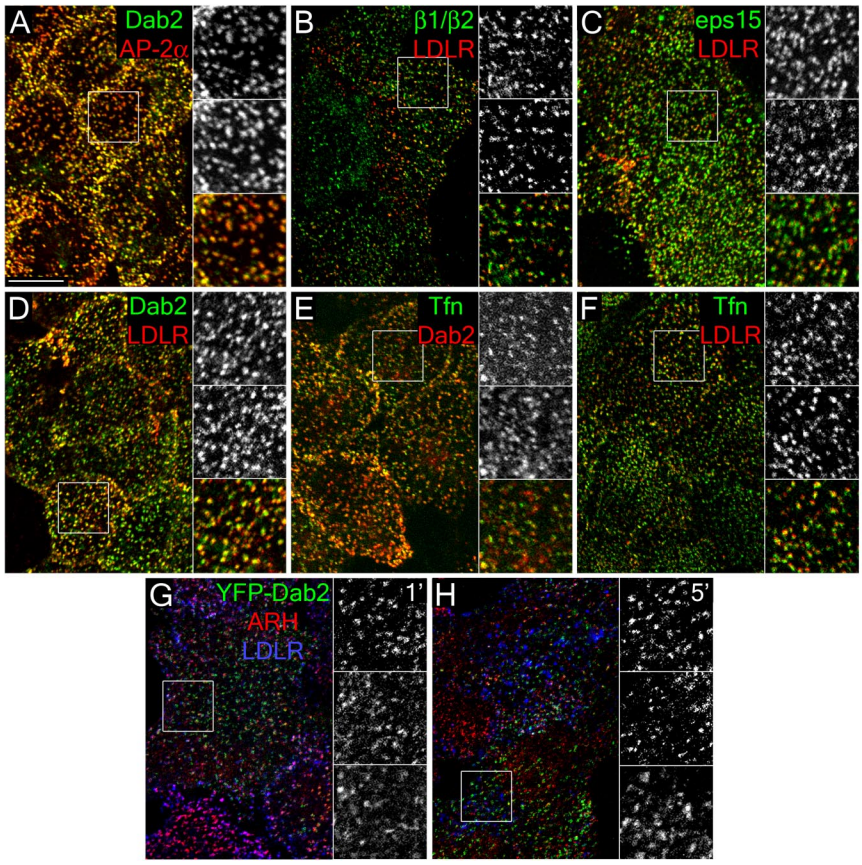

Figure 7. General localization of CLASPs and LDL receptors to endocytic coated coats at steady state. HeLa SS6 cells cultured in DMEM containing 10% LPDS overnight were either fixed and stained with anti-Dab2 antibody and anti-AP-2 α subunit mAb AP.6 (A), or surface-labeled with anti-LDL receptor mAb IgG-C7 (LDLR), fixed and stained with either affinity-purified anti-AP-1/2 $\beta1/\beta2$-subunit GD/1 (B), anti-eps15 (C), or anti-Dab2 (D) antibodies, or surface-labeled with Tfn488 (Tfn), fixed and stained with anti-Dab2 antibody (E), or surface-labeled with both Tfn488 and anti-LDL receptor mAb IgG-C7 (F). Representative single confocal optical sections are shown with color-separated and merged magnifications of each boxed region shown on the right. Alternatively, HeLa SS6 cells transfected with YFP-Dab2 were incubated with anti-LDL receptor mAb IgG-C7 for 1 (G) or 5 min (H) at 37°C, fixed, and stained with anti-ARH antibody. Scale bar, 10 μm.

rather ushering LDL receptors through pre-existing coated buds. One prediction of this idea is that ARH requires AP-2 for localization to clathrin bud sites. Indeed, in AP-2+Dab2 knocked-down cells, but not with AP-2 or Dab2 knockdown alone, both transferrin and LDL receptor internalization is impaired despite normal ARH levels (Figure 6F). In these uptake experiments, fluorescent ligands are added directly to cells at 37°C, and in the AP-2–depleted cells (Figure 6B), transferrin, but not LDL, is poorly internalized and accumulates diffusely over the cell surface. Consistent with the ability of Dab2 to polymerize clathrin (Mishra *et al.*, 2002a) and drive LDL receptor internalization (Morris *et al.*, 2002; Maurer and Cooper, 2005), Dab2 does not exhibit a requirement for AP-2; knockdown of ARH+AP-2 dramatically impairs transferrin but not LDL receptor internalization (Figure 6E). Taken altogether, these experiments clearly reveal important differences in the molecular mode of operation of these two CLASPs: like β-arrestin, ARH operates by directing LDL receptors to pre-existing clathrin-coated structures containing AP-2, whereas Dab2 can sustain clathrin-dependent LDL internalization independent of AP-2.

Dab2 Populates the Majority of Surface Clathrin Structures

If Dab2 can maintain LDL endocytosis independent of AP-2, it is possible that this CLASP nucleates discrete clathrin coats, allowing different cargo types to be internalized within different subpopulations of coated vesicles, a possibility already suggested for certain G protein–coupled receptors (GPCRs) (Cao *et al.*, 1998), transferrin (Tosoni *et al.*, 2005), and LDL (Lakadamyali *et al.*, 2006) receptors. In this case, Dab2 should only be present within a select subpopulation of coated structures along with the respective cargo. However, in both normal and ARH$^{-/-}$ fibroblasts at steady state, AP-2 is present in 92% of surface-proximal clathrin structures, Dab2 in 82%, and Dab2 populates 92% of the AP-2–positive structures (Figure 1 and Supplementary Figure S5; Morris and Cooper, 2001). Essentially analogous results are observed with HeLa and CV-1 cells (Figure 7, A and B, and unpublished data), clearly discrepant with the reported distribution of Dab2 in BS-C-1 cells (Lakadamyali *et al.*, 2006), which, like CV-1 cells, are derived from the African green monkey (see below). Freeze-etch EM reveals Dab2 positioned within the majority of clathrin structures at the plasma membrane. Frequently, the CLASP appears positioned near the edges of the lattice (Figure 8), like eps15 (Tebar *et al.*, 1996; Edeling *et al.*, 2006), a Dab2-binding partner, although immunogold Dab2 labeling is also seen within regions of assembled lattice and on buds, particularly in HeLa cells. The predominantly coat-associated distribution of Dab2 is similar to the near-perfect colocalization observed for either eps15 or epsin in HeLa, CHO, and A431 cells (Chen *et al.*, 1998; Yim *et al.*, 2005; Hawryluk *et al.*, 2006).

Moreover, the distribution of Dab2 is paralleled by the LDL receptor; the vast majority (84–89%) of surface LDL (and transferrin; 89–93%) is found in Dab2-positive puncta (Figure 7 and Supplementary Figure S5). In fibroblasts, 77% of ARH-positive puncta are positive for the LDL receptor and, at steady state, LDL, transferrin and clathrin signals are also highly coincident in both HeLa cells and fibroblasts; 88% of clathrin light-chain–positive structures contain transferrin, 81% contain LDL, and 56% have both transferrin and LDL signals when fibroblasts are labeled simultaneously with both ligands on ice (Figure 7 and Supplementary Fig-

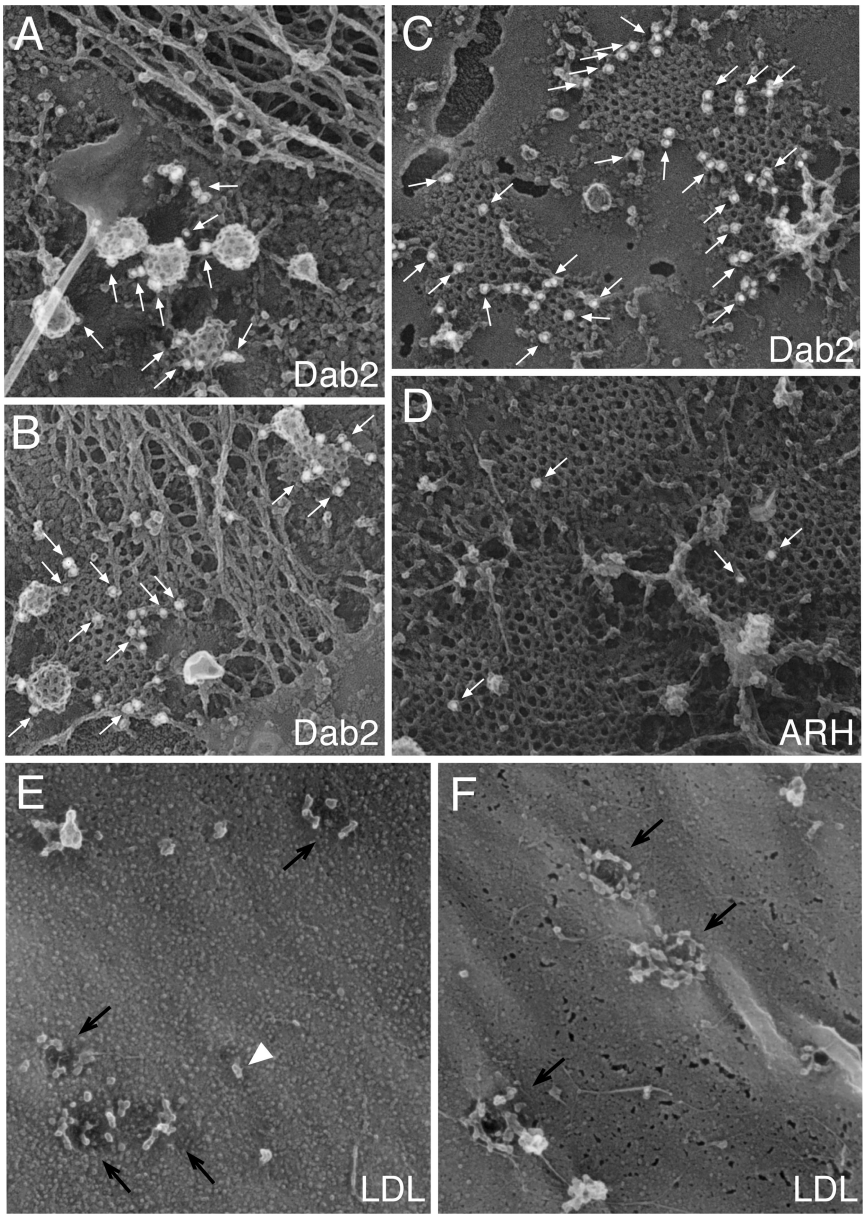

Figure 8. Ultrastructural localization of Dab2, ARH, and LDL in clathrin coats. (A–F) Fixed plasma membrane sheets prepared from control GM01386 fibroblasts (A, D, and E) or HeLa cells (B, C, and F) were labeled with either affinity-purified anti-Dab2 or ARH antibodies, and then with secondary antibodies conjugated to 15-nm colloidal-gold particles. Individual gold particles appear as white spheres (arrows), and representative freeze-etch images show the spatial distribution of endogenous Dab2 and ARH. (E and F) Control fibroblasts (GM01386, E) or HeLa cells (F) incubated in 10% LPDS for 24 h were incubated with 50 μg/ml LDL at either 0°C (F) or 37°C (E) and fixed before preparation of replicas of the external cell surface. Individual LDL particles (arrowheads) and invaginated pits (arrows) are indicated.

ure S5). On adding LDL to cells at 37°C, YFP-Dab2 and endogenous ARH colocalize with LDL receptors during the initial period of LDL uptake, but diverge within 5 min (Figure 7, G and H). Also, in HeLa cells, 95% of eps15-positive structures contain LDL receptors (Figure 7C), again attesting to the occurrence of numerous CLASPs within a single assembling coat.

EM views of replicas of the external surface of fibroblasts show oval, ~25-nm LDL particles clustered around and within invaginations (coated buds; Figure 8E; Heuser, 1980; Sanan *et al.*, 1987; Heuser and Anderson, 1989). HeLa cells, too, have LDL massed at presumptive bud site invaginations (Figure 8F). We also note that the extent of LDL receptor up-regulation upon culture in lipoprotein-deficient serum is not uniform in all cells, so adjacent cells often display different LDL receptor densities at the surface (Figures 7B and 10D). Dab2 is nevertheless distributed throughout surface clathrin structures and, indeed, there is little difference in the subcellular distribution of Dab2 between cells grown in whole or lipoprotein-deficient serum (Supplementary Figure S5). In sum, at least for constitutively endocytosed receptors, we find little evidence of obvious compartmentalization of incoming cargo within functionally distinct surface clathrin-coated structures, and the localization of FXNPXY-recognizing CLASPs to endocytic coats appears independent of receptor level fluctuations.

Spatiotemporal Analysis of CLASPs during LDL Internalization

The small dispersed surface puncta that transiently overexpressed YFP-Dab2 and ARH-GFP both localize to in HeLa cells (Figures 5 and 7) contain AP-2 and clathrin (unpublished data). In these structures, the recovery of Y/GFP fluorescence after photobleaching reinforces the adaptor-like properties of these CLASPs (Figure 9, A and B). YFP-Dab2 repopulates bleached puncta with a $t_{1/2}$ of ~15 s, analogous to clathrin and AP-2 (Wu *et al.*, 2001, 2003), whereas ARH-GFP recovers slightly quicker ($t_{1/2}$ =

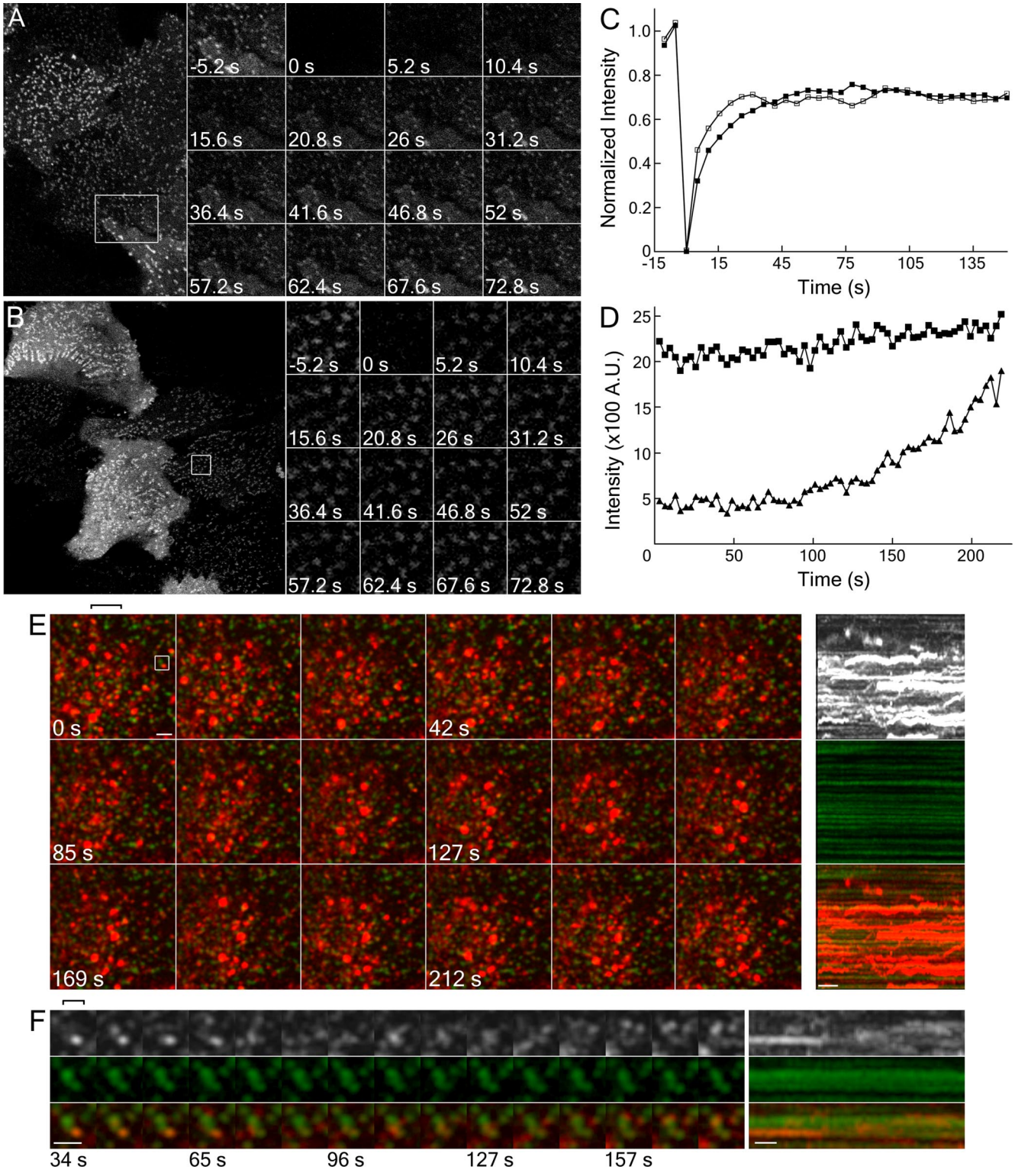

Figure 9. Live cell dynamics of Dab2 and ARH. HeLa cells transiently transfected with either YFP-Dab2 (A) or ARH-GFP (B) were photobleached (boxed region) with a 405-nm laser at time 0 and imaged every 5.2 s to follow recovery of the fluorescent signal. Magnified views of the bleached region at the indicated times are shown in the insets. (C) Normalized fluorescence intensity of YFP-Dab2 (14 separate cells, ■) and ARH-GFP (29 separate cells, □) within the bleached regions. (D–F) YFP-Dab2 (middle panels, green) transfected HeLa cells were grown in LPDS overnight, incubated with 4 μg/ml DiI-LDL (top panels, red) and imaged every 3.3 (D) or 3.4 s (E and F) either during LDL addition (D) or 21 min later (E and F). (D) Quantitation of the fluorescence intensity of 17 structures during early time points shows that the intensity of LDL (▲) accumulates in these Dab2-positive structures (■). The averaged intensity for Dab2 and LDL in all these structures is shown. (E and F) At later time points, the internalized DiI-LDL has moved to larger, brighter YFP-Dab2-negative endosomal compartments, though LDL still accumulates and internalizes from surface Dab2-positive structures. Importantly, the concentration of LDL used in these experiments is ~10-fold below the saturating concentration at 37°C (>50 μg/ml; Brown and Goldstein, 1986), so only a subset of surface LDL receptors are marked with fluorescent ligand.

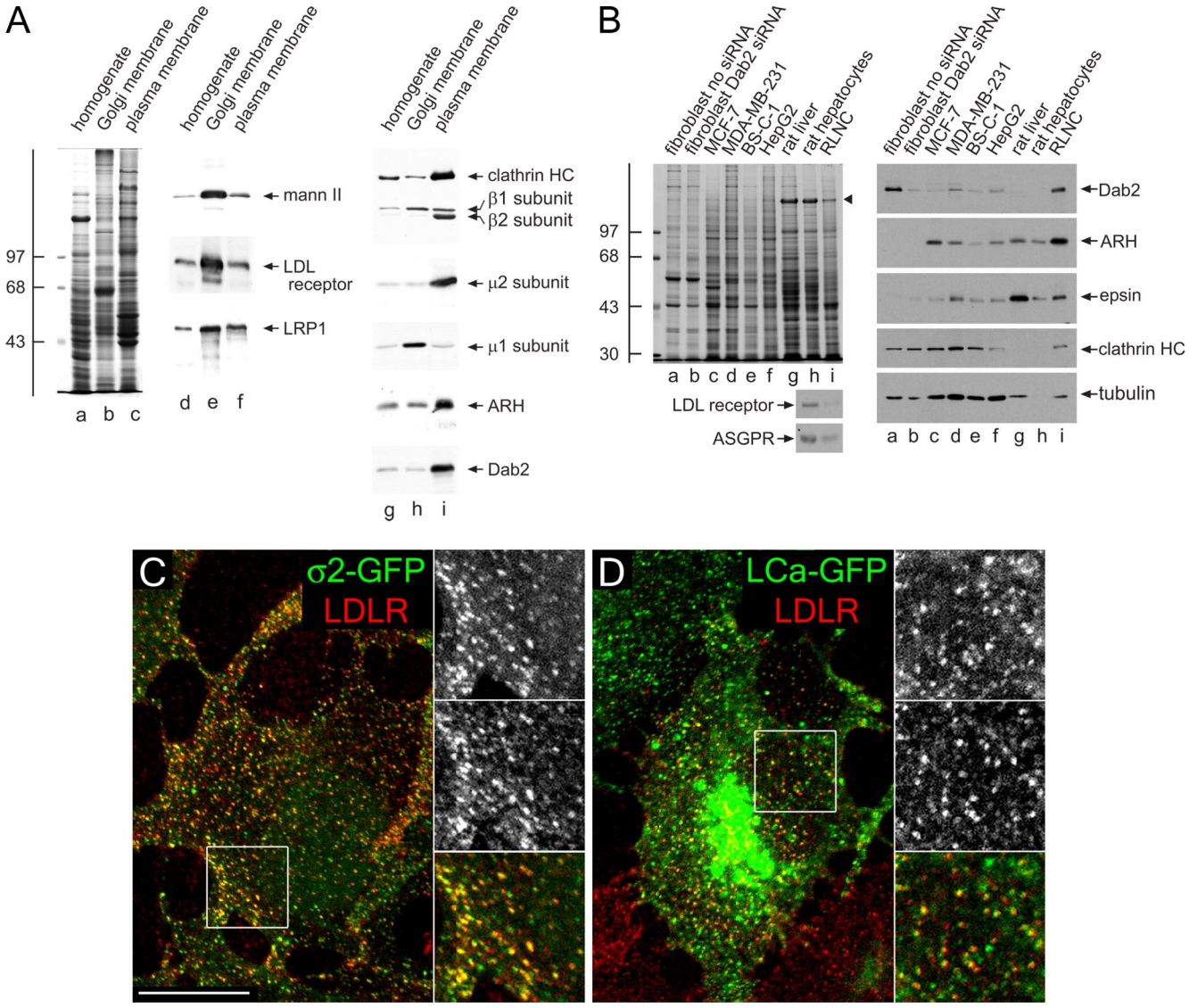

Figure 10. Cell-type-specific expression of Dab2 in the liver. (A) Samples of 25 μg of rat liver homogenate (lanes a, d, and g), purified rat liver Golgi membranes (lanes b, e, and h), or rat liver plasma membrane sheets (lane c, f and i) were resolved by SDS-PAGE and either stained with Coomassie blue (lane a–c) or transferred to nitrocellulose (lanes d–i). Portions of replicate blots were probed with antibodies directed against α-mannosidase II (mann II), the LDL receptor, LRP1, clathrin heavy chain (HC), AP-1/2 β1/β2 subunits, AP-2 μ2 subunit, AP-1 μ1 subunit, ARH, or Dab2. The position of the molecular mass standards (in kDa) is indicated on the left. (B) Lysates from ARH$^{-/-}$ fibroblasts either mock (lane a) transfected or transfected with Dab2 siRNA (lane b), MCF-7 (lane c), MDA-MB-231 (lane d), BS-C-1 (lane e), or HepG2 (lane f) cultured cell lines, rat liver homogenate (lane g), rat hepatocyte (lane h), or rat liver nonhepatocyte cell (RLNC, lane i) lysates were resolved by SDS-PAGE under reducing (top left, right panels) or nonreducing (bottom left panels) conditions and stained with Coomassie blue (top left) or transferred to nitrocellulose. A major 180-kDa hepatic polypeptide that prevents efficient transfer of the clathrin heavy chain onto nitrocellulose is indicated on the stained gel (arrowhead). Relevant portions of the blots were probed with affinity-purified anti-Dab2, anti-ARH, anti-epsin or rat-specific anti-LDL receptor polyclonal antibodies, or anti-clathrin HC mAb TD.1, anti-tubulin mAb E7, or anti-asialoglycoprotein receptor mAb 8D7. Analogous results are obtained using an independent goat anti-Dab2 antibody (unpublished data). (C and D) BS-C-1 cells stably expressing either AP-2 σ2-GFP (C, green) or clathrin LCa-GFP (D, green) were grown overnight in DMEM containing LPDS, surface labeled with anti-LDL receptor mAb C7 (LDLR, red) on ice. Representative single confocal optical sections of fixed cells are shown with color-separated and merged magnifications of each boxed region shown on the right. Scale bar, 10 μm.

Figure 9 (Cont). A cluster of selected surface YFP-Dab2 structures containing LDL, indicated with the rectangle in E, is magnified in F. Separation of the DiI-LDL signal from the Dab2-YFP and local movement of the internalized vesicle are evident. E and F are from Supplementary Movie 2. The brackets indicate the vertical position from each image set used to generate the kymograph. Scale bar, 10 μm in A and B, 1 μm in E, and 500 nm in F. Kymograph scale bar, 20 s. Note the striking differences in the dynamics of the Dab2-YFP and DiI-LDL structures seen in the kymographs.

~9 s; Figure 9C). Typically, >85% of the prebleach puncta rapidly reacquire up to ~70% of the initial fluorescence in these experiments, consistent with both Dab2 and ARH cycling between soluble and membrane-bound states. Yet, despite dynamic oscillation of Dab2 and ARH at bud sites, many surface structures appear comparatively immobile over time, a behavior typically observed for tagged clathrin, AP-2, and other endocytic components (Gaidarov *et al.*, 1999;

Rappoport *et al.,* 2003; Keyel *et al.,* 2004; Merrifield *et al.,* 2005; Bellve *et al.,* 2006) but which, nonetheless, correlate with endocytic uptake (Bellve *et al.,* 2006). In time-resolved images of transiently transfected HeLa cells, added DiI-LDL initially clusters at YFP-Dab2–positive surface puncta, whereas 5–20 min later, internalized LDL within larger, mobile endosomes is not colocalized with Dab2 (Figure 9E; Supplementary Movie 2); instead, rapid lateral LDL translocations indicative of directed endosome movement are apparent (Supplementary Movie 2 and Figure 9E, kymograph). Consequently, we judge the small, relatively immobile spots to be coats assembling at the plasma membrane. Similar DiI-LDL-containing clusters are seen in HeLa cells expressing ARH-GFP, GFP-epsin 1, or GFP-clathrin light chain (LCa; unpublished data), verifying the surface positioning these structures and, again, showing LDL concentrates in clathrin regions containing various CLASPs. At these small peripheral structures, LDL can be seen to accumulate within a minute or two after addition of DiI-LDL (Figure 9, D and E) and, in general, LDL concentrates in these puncta (Figure 9D).

The temporal relationship between Dab2 and LDL in our data sets can be categorized into what appear to be distinct types of budding events. For example, occasions where both Dab2 and LDL signals disappear from the optical section simultaneously occur. More frequently, overlapping Dab2- and LDL-positive puncta separate, and the Dab2 signal is lost rapidly revealing an LDL-positive endocytic vesicle (Figure 9F), which moves locally and often fuses with an adjacent vesicle. Also noticeable are larger LDL-rich endosomes moving close to the plasma membrane surface that consume local cargo emerging from assembled Dab2 zones (Supplementary Movie 2). The behavior of these structures is strikingly reminiscent of the consumption of just internalized endocytic vesicles by actin-dependent directed-movement of cargo-laden endosomal vesicles recently reported in *Saccharomyces cerevisiae* (Toshima *et al.,* 2006). Altogether, our imaging studies confirm that the spatiotemporal behavior of Dab2 and ARH is consistent with a proposed role as FXNPXY-selective CLASPs. Further, the data reveal a dense subsurface population of dynamic, LDL-positive transport vesicles and a substantial degree of rapid homogenization/intermingling of the internalized ligand within early sorting endosomes.

Regulated Dab2 Expression in Hepatocytes

Finally, if Dab2 and ARH are both generally present in surface coated buds and can operate analogously to promote LDL receptor internalization, why is ARH so crucial for maintaining normal plasma levels of LDL in vivo? One potential explanation is tissue-specific expression patterns of Dab2 and ARH. Comparisons of rat liver homogenate, purified Golgi membranes, and isolated plasma membrane sheets show dramatically different overall protein compositions (Figure 10A, lanes a–c) and the expected enrichment of AP-1 at the Golgi and AP-2 on the plasma membrane (Figure 10A, lanes g–i). However, both Dab2 and ARH are similarly enriched within the isolated plasma membrane preparation. These sheets are purified from whole liver homogenates (Hubbard *et al.,* 1983), but when separated hepatocyte and nonhepatocyte fractions are compared, Dab2 is strikingly absent from asialoglycoprotein receptor–positive hepatocytes, although the CLASP is well expressed in the nonparenchymal (Kupffer, sinusoidal endothelial, and hepatic stellate cells) fraction (Figure 10B). By contrast, ARH and epsin 1 are present in both populations. Purified rat hepatocytes express less Dab2 protein at steady state than previously characterized cultured cell lines with down-regulated Dab2 (MDA-MB-231 and MCF-7; Fazili *et al.,* 1999), although, again, ARH levels are roughly comparable. Also of note, HepG2, a human hepatoma line and BS-C-1 cells also contain low relative levels of Dab2 (Figure 10B). Yet, in our experiments, BS-C-1 cells still cluster LDL receptors at the majority AP-2 (σ2-GFP)-containing structures (Figure 9C), and at many surface clathrin (LCa-GFP) puncta (Figure 10D). These results again reinforce the redundancy between ARH and Dab2 and differ from a recent report showing only ~30% of surface clathrin structures associated with labeled LDL in BS-C-1 cells (Lakadamyali *et al.,* 2006). We conclude that since the vast majority of plasma LDL is cleared/degraded by hepatocytes in vivo (Osono *et al.,* 1995), the exceedingly low level of Dab2 present in this cell type is fully consistent with the phenotype that results from inheritance of two mutant ARH alleles; although nonparenchymal cells may be able to internalize LDL in an $ARH^{-/-}$ background, hepatocytes are clearly unlikely to internalize FXNPXY signals normally.

DISCUSSION

Clathrin-coated vesicles are high-capacity carriers that efficiently shuttle numerous cargo types into the cell interior in a generally noncompetitive manner (Marks *et al.,* 1996; Santini *et al.,* 1998; Warren *et al.,* 1998). Although it is well accepted that cargo selection depends upon adaptors, here we provide functional evidence that efficient internalization of the LDL receptor is only indirectly dependent on the AP-2 adaptor and can, if driven by Dab2, occur in the absence of the heterotetramer. Thus, our experiments formally validate the CLASP hypothesis (Traub, 2003; Robinson, 2004; Sorkin, 2004) and lead to three major conclusions. First, the FXNPXY-selective CLASPs ARH and Dab2 operate in a functionally redundant manner, despite engaging the clathrin coat machinery in molecularly distinct ways; these proteins operate analogously to, and in parallel with, AP-2–dependent sequestration of transferrin receptors (Hinrichsen *et al.,* 2003; Motley *et al.,* 2003) and epsin/eps15/eps15R-mediated sorting of poly/multiubiquitinated proteins (Barriere *et al.,* 2006; Duncan *et al.,* 2006; Hawryluk *et al.,* 2006; Wang *et al.,* 2006). Very similar results revealing both the cargo selectivity and functional redundancy of ARH and Dab2 have been obtained in two independent studies (Maurer and Cooper, 2006; Anne Soutar, personal communication). Second, when Dab2 is present at "normal" cellular levels, the CLASP generally populates most clathrin-coated structures along with AP-2, epsin, and eps15, independent of LDL receptor expression levels. Third, Dab2 expression is cell type specific and, consequently, appears to underlie the hypercholesterolemic phenotype observed in both ARH-nullizygous patients and mice.

Given the selectivity and ability of certain CLASPs to sustain clathrin-mediated endocytosis in the absence of AP-2, refined models positing biased sorting of different cargo classes into discrete subpopulations of surface clathrin coats have been proposed (Tosoni *et al.,* 2005; Lakadamyali *et al.,* 2006). We believe that CLASPs are unlikely to target/generate distinct populations of clathrin coats for several reasons. First, classic EM studies document the colocalization of various cargo within single budding profiles at the plasma membrane: for example, LDL and α_2-macroglobulin (LRP1; Via *et al.,* 1982), transferrin and asialoglycoprotein (Neutra *et al.,* 1985; Stoorvogel *et al.,* 1987), lysosomal hydrolases (mannose 6-phosphate receptor), and α_2-macroglobulin (Willingham *et al.,* 1981), LDL and EGF (Carpentier *et al.,*

1982), EGF and transferrin (Hanover *et al.*, 1984), and EGF and α_2-macroglobulin or adenovirus (Willingham *et al.*, 1983). Further, active segregation of CLASPs and cargo would certainly require energy but, as most cargo sorted by clathrin-mediated events converge in a common early endosome population (Ajioka and Kaplan, 1987; Dunn *et al.*, 1989; Maxfield and McGraw, 2004), any advantage of presorting various cargo would evidently be eliminated. In nonpolarized cells, peripheral Rab5-positive LDL-containing early endosomes mature by fusing with other Rab5- and transferrin/LDL-positive structures; homotypic fusion is estimated to occur once or twice per minute as early endosomes expand in size over ~10–15 min, mingling incoming endocytic vesicle contents (Rink *et al.*, 2005). Rab4-containing tubules emanate from these early endosomes, allowing transferrin to exit, whereas LDL (and other molecules destined for degradation) concentrates within the vacuolar portion of the sorting endosome. There is a replete literature showing that LDL, asialoglycoprotein, and transferrin initially enter common sorting endosomes and segregate with a $t_{1/2}$ of ~2.5 min (Stoorvogel *et al.*, 1987; Dunn *et al.*, 1989; Ghosh *et al.*, 1994; Maxfield and McGraw, 2004), and the combined data have been synthesized into a general model for the iterative processing of cargo types that accompanies endosome maturation (Maxfield and McGraw, 2004). The enlarged LDL-positive late endosomes that ensue (Figures 3 and 9; Supplementary Movie 2) must mean that LDL-carrying structures fuse together as the endosome transits toward the lysosome and converts to a Rab7-positive stage. The time frame of this transition from small Rab5-positive to large Rab7-positive endosomes is ~20–40 min (Ghosh *et al.*, 1994; Rink *et al.*, 2005), in excellent agreement with classic data showing that detection of LDL degradation products requires >30 min after initial internalization (Brown and Goldstein, 1986). With this general and extensively substantiated model for endosome maturation along the degradative pathway, the teleological benefit of targeting a population of LDL-laden coated vesicles to a Rab7-positive status within only a few minutes (Lakadamyali *et al.*, 2006) is not at all obvious to us. In this regard, it is also worth noting that although LDL moves to the late endosome for catabolism, the LDL receptor has a long biological life (~20 h) and follows a different trajectory, recycling back to the surface roughly five or six times per hour in fibroblasts (Brown and Goldstein, 1986), similar to the transferrin receptor. Furthermore, the slowed progression of LDL toward the late endosome reported after EGF stimulation (Rink *et al.*, 2005) tends again to argue against compositionally distinct partitioning of LDL into a subset of clathrin structures at the cell surface.

Perhaps a more serious concern with the general idea of cargo-specific coats at the plasma membrane is that we believe there is currently no plausible mechanistic basis for their formation. Cargo-selective CLASPs, including β-arrestins, epsin, ARH, and Dab2, bind with relatively high-affinity to clathrin and PtdIns(4,5)P_2, general components of all surface clathrin structures, as well as to AP-2. The membrane and cytosolic pools of these adaptors exchange rapidly, with a $t_{1/2}$ of ~15 s (Figure 9; Wu *et al.*, 2003; Yim *et al.*, 2005), permitting soluble adaptors to interchange repeatedly at each clathrin bud during its 20–90-s lifetime (Gaidarov *et al.*, 1999; Merrifield *et al.*, 2002; Wu *et al.*, 2003). Therefore, an ongoing and efficient segregation mechanism would be necessary to ensure the conversion of random CLASP encounters with assembling lattices into differential patterning of CLASPs within only a subset of coats, rather than in all of them. Yet, several time-resolved imaging studies demonstrate that fluorescently tagged β-arrestins populate virtually all detectable clathrin structures at the surface after ligand activation of a suitable GPCR (Santini *et al.*, 2002; Scott *et al.*, 2002). ARH accesses clathrin coats in a manner strictly analogous to β-arrestins, by binding to the AP-2 β2 appendage platform and the clathrin heavy chain terminal domain. Indeed, ectopically expressed ARH-GFP is found in the majority of clathrin structures on the surface (Figure 9B). Thus, our current understanding of the dynamics and points of contact between CLASPs and the core clathrin machinery makes the assembly and maintenance of compositionally distinct buds improbable in our view and is clearly inconsistent with the steady state distribution of Dab2 (Morris and Cooper, 2001), ARH, surface LDL receptors (Anderson *et al.*, 1978; Heuser and Anderson, 1989; Sanan and Anderson, 1991), and epsin 1 (Chen *et al.*, 1998; Yim *et al.*, 2005; Hawryluk *et al.*, 2006) in several cell types.

Instead, our data show specifically that Dab2 is present in the majority of clathrin structures at the surface, consequently allowing clustering of LDL. We cannot, however, rule out that under some circumstances, regulation of CLASP cargo-engagement properties, perhaps by phosphorylation as occurs with AP-2 (Olusanya *et al.*, 2001; Höning *et al.*, 2005), limits the composition of single clathrin buds by focally disabling certain CLASPs within the assembled coat. It is also conceivable that massed cargo could stabilize CLASPs in the assembly zone to generate cargo-selective buds, but this would apparently require preferential entry of transmembrane cargo into specific, but not all, coat-forming regions on the plasma membrane. Yet, LDL receptors are seemingly dispersed randomly over the surface membrane upon reinsertion from recycling endocytic vesicles, as are internalization-defective LDL receptors (Sanan *et al.*, 1987). Our deep-etch images reveal that Dab2 is frequently positioned around the rims of the clathrin lattice. This may be due, in part, to association of Dab2 with eps15, which is almost exclusively positioned at lattice edges (Tebar *et al.*, 1996; Edeling *et al.*, 2006). Similar visualization of LDL particles on the extracellular plasma membrane surface (Heuser, 1980; Sanan *et al.*, 1987; Heuser and Anderson, 1989; Sanan and Anderson, 1991), as well as thin section analysis (Orci *et al.*, 1978; Handley *et al.*, 1981; Paavola *et al.*, 1985), often shows clustered peripheral LDL particles, positioned circumferentially around the involuting bud (Figure 8). Although we cannot rule out that epitope masking reduces detection of Dab2 within the lattice interior, it is probable this peripheral clustering of LDL is due to deposition of Dab2 near the edges. Our live cell data show some YFP-Dab2 does, on occasion, accompany LDL on a budding vesicle, and we also do observe some Dab2 labeling within the lattice, on invaginating buds, and in coated vesicle preparations (Hawryluk *et al.*, 2006). ARH, on the other hand, appears to be found predominantly in the interior of clathrin lattices, occasionally on invaginating regions. Although the density of ARH labeling is low, this finding is consistent with ARH and β-arrestin playing similar roles and β-arrestin being enriched in preparations of purified coated vesicles (Blondeau *et al.*, 2004). In time-resolved studies, the majority of the YFP-Dab2 signal at surface puncta is relatively immobile, in accord with other endocytic proteins (Rappoport *et al.*, 2003; Keyel *et al.*, 2004; Bellve *et al.*, 2006) and recent work in primary adipocytes (Bellve *et al.*, 2006). Indeed extensive arrays of flat hexagonal clathrin lattice are not only found on the ventral surface of normal human fibroblasts (Heuser, 1980; Heuser and Anderson, 1989), but on the dorsal surface as well (Damke *et al.*, 1994), where LDL is similarly enriched around the circumference of the clathrin assemblies (Sanan and Anderson, 1991). Thus, in cells where

extensive arrays of clathrin occur, Dab2 may locally concentrate FXNPXY cargo molecules, like the LDL receptor, for packaging into buds that form within or at the periphery these extended lattices.

There are at least two mammalian tissues where functional redundancy between Dab2 and ARH appears to have been selected against. Hepatocytes do not express Dab2 in sufficient quantity to bypass ARH loss and, reciprocally, during embryonic development the visceral endoderm does not appear to express ARH (Maurer and Cooper, 2005) and, consequently, targeted gene disruption of Dab2 is homozygous lethal (Morris *et al.*, 2002). Hepatocytes characteristically respond to liver damage or partial hepatectomy with rapid proliferation and remodeling to restore the functional capability and mass of the liver. Because Dab2 acts downstream of TGF-β receptors to promote SMAD activation (Hocevar *et al.*, 2001), and hepatocyte DNA synthesis and proliferation is potently suppressed by TGF-β (Wollenberg *et al.*, 1987), perhaps the very low level of Dab2 in parenchymal cells is functionally related to the intrinsic proliferative capacity of hepatocytes.

ACKNOWLEDGMENTS

We are extremely grateful to William Bowen, Jr. for generously providing rat hepatocyte fractions, to our numerous colleagues who provided important reagents, to Jon Cooper and Anne Soutar for sharing unpublished results, to members of the Traub lab for critical reading of the manuscript, and to Stuart Kornfeld for insightful advice and suggestions. This work was funded by National Institutes of Health Grant R01 DK53249 and American Heart Association (AHA) Established Investigator Award (0540007N) to L.M.T. P.A.K. was supported by AHA Predoctoral Fellowship Award 0415428U.

REFERENCES

Ahle, S., Mann, A., Eichelsbacher, U., and Ungewickell, U. (1988). Structural relationships between clathrin assembly proteins from the Golgi and the plasma membrane. EMBO J. *7*, 919–929.

Ajioka, R. S., and Kaplan, J. (1987). Characterization of endocytic compartments using the horseradish peroxidase-diaminobenzidine density shift technique. J. Cell Biol. *104*, 77–85.

Anderson, R. G., Vasile, E., Mello, R. J., Brown, M. S., and Goldstein, J. L. (1978). Immunocytochemical visualization of coated pits and vesicles in human fibroblasts: relation to low density lipoprotein receptor distribution. Cell *15*, 919–933.

Arca, M., *et al.* (2002). Autosomal recessive hypercholesterolaemia in Sardinia, Italy, and mutations in ARH: a clinical and molecular genetic analysis. Lancet *359*, 841–847.

Barriere, H., Nemes, C., Lechardeur, D., Khan-Mohammad, M., Fruh, K., and Lukacs, G. L. (2006). Molecular basis of Ub-dependent internalization of membrane proteins in mammalian cells. Traffic *7*, 282–297.

Bellve, K. D., Leonard, D., Standley, C., Lifshitz, L. M., Tuft, R. A., Hayakawa, A., Corvera, S., and Fogarty, K. E. (2006). Plasma membrane domains specialized for clathrin-mediated endocytosis in primary cells. J. Biol. Chem. *281*, 16139–16146.

Blondeau, F., *et al.* (2004). Tandem MS analysis of brain clathrin-coated vesicles reveals their critical involvement in synaptic vesicle recycling. Proc. Natl. Acad. Sci. USA *101*, 3833–3838.

Bonifacino, J. S., and Traub, L. M. (2003). Signals for sorting of transmembrane proteins to endosomes and lysosomes. Annu. Rev. Biochem. *72*, 395–447.

Breitfeld, P. P., Casanova, J. E., Harris, J. M., Simister, N. E., and Mostov, K. E. (1989). Expression and analysis of the polymeric immunoglobulin receptor in Madin-Darby canine kidney cells using retroviral vectors. Methods Cell Biol. *32*, 329–337.

Brodsky, F. M. (1985). Clathrin structure characterized with monoclonal antibodies. II. Identification of in vivo forms of clathrin. J. Cell Biol. *101*, 2055–2062.

Brown, M. S., and Goldstein, J. L. (1986). A receptor-mediated pathway for cholesterol homeostasis. Science *232*, 34–47.

Cao, T. T., Mays, R. W., and von Zastrow, M. (1998). Regulated endocytosis of G-protein-coupled receptors by a biochemically and functionally distinct subpopulation of clathrin-coated pits. J. Biol. Chem. *273*, 24592–24602.

Carpentier, J. L., Gorden, P., Anderson, R. G., Goldstein, J. L., Brown, M. S., Cohen, S., and Orci, L. (1982). Co-localization of ^{125}I-epidermal growth factor and ferritin-low density lipoprotein in coated pits: a quantitative electron microscopic study in normal and mutant human fibroblasts. J. Cell Biol. *95*, 73–77.

Chen, H., Fre, S., Slepnev, V. I., Capua, M. R., Takei, K., Butler, M. H., Di Fiore, P. P., and De Camilli, P. (1998). Epsin is an EH-domain-binding protein implicated in clathrin-mediated endocytosis. Nature *394*, 793–797.

Chen, W. J., Goldstein, J. L., and Brown, M. S. (1990). NPXY, a sequence often found in cytoplasmic tails, is required for coated pit-mediated internalization of the low density lipoprotein receptor. J. Biol. Chem. *265*, 3116–3123.

Chin, D. J., Straubinger, R. M., Acton, S., Nathke, I., and Brodsky, F. M. (1989). 100-kDa polypeptides in peripheral clathrin-coated vesicles are required for receptor-mediated endocytosis. Proc. Natl. Acad. Sci. USA *86*, 9289–9293.

Cuitino, L., Matute, R., Retamal, C., Bu, G., Inestrosa, N. C., and Marzolo, M. P. (2005). ApoER2 is endocytosed by a clathrin-mediated process involving the adaptor protein Dab2 independent of its rafts' association. Traffic *6*, 820–838.

Damke, H., Baba, T., Warnock, D. E., and Schmid, S. L. (1994). Induction of mutant dynamin specifically blocks endocytic coated vesicle formation. J. Cell Biol. *127*, 915–934.

Davis, C. G., Lehrman, M. A., Russell, D. W., Anderson, R. G., Brown, M. S., and Goldstein, J. L. (1986). The J.D. mutation in familial hypercholesterolemia: amino acid substitution in cytoplasmic domain impedes internalization of LDL receptors. Cell *45*, 15–24.

Davis, C. G., van Driel, I. R., Russell, D. W., Brown, M. S., and Goldstein, J. L. (1987). The low density lipoprotein receptor. Identification of amino acids in cytoplasmic domain required for rapid endocytosis. J. Biol. Chem. *262*, 4075–4082.

Drake, M. T., Downs, M. A., and Traub, L. M. (2000). Epsin binds to clathrin by associating directly with the clathrin-terminal domain: evidence for cooperative binding through two discrete sites. J. Biol. Chem. *275*, 6479–6489.

Duncan, L. M., Piper, S., Dodd, R. B., Saville, M. K., Sanderson, C. M., Luzio, J. P., and Lehner, P. J. (2006). Lysine-63 linked ubiquitination is required for endolysosomal degradation of class I molecules. EMBO J. *25*, 1635–1645.

Dunn, K. W., McGraw, T. E., and Maxfield, F. R. (1989). Iterative fractionation of recycling receptors from lysosomally destined ligands in an early sorting endosome. J. Cell Biol. *109*, 3303–3314.

Edeling, M. A., Mishra, S. K., Keyel, P. A., Steinhauser, A. L., Collins, B. M., Roth, R., Heuser, J. E., Owen, D. J., and Traub, L. M. (2006). Molecular switches involving the AP-2 β2 appendage regulate endocytic cargo selection and clathrin coat assembly. Dev. Cell *10*, 329–342.

Eden, E. R., Patel, D. D., Sun, X., Burden, J. J., Themis, M., Edwards, M., Lee, P., Neuwirth, C., Naoumova, R. P., and Soutar, A. K. (2002). Restoration of LDL-receptor function in cells from patients with autosomal recessive hypercholesterolemia by retroviral expression of *ARH1*. J. Clin. Invest. *110*, 1695–1702.

Fazili, Z., Sun, W., Mittelstaedt, S., Cohen, C., and Xu, X .X. (1999). Disabled-2 inactivation is an early step in ovarian tumorigenicity. Oncogene *18*, 3104–3113.

Gaidarov, I., Santini, F., Warren, R. A., and Keen, J. H. (1999). Spatial control of coated-pit dynamics in living cells. Nat. Cell Biol. *1*, 1–7.

Garcia, C. K., *et al.* (2001). Autosomal recessive hypercholesterolemia caused by mutations in a putative LDL receptor adaptor protein. Science *292*, 1394–1398.

Garuti, R., Jones, C., Li, W. P., Michaely, P., Herz, J., Gerard, R. D., Cohen, J. C., and Hobbs, H. H. (2005). The modular adaptor protein autosomal recessive hypercholesterolemia (ARH) promotes low density lipoprotein receptor clustering into clathrin-coated pits. J. Biol. Chem. *280*, 40996–41004.

Ghosh, R. N., Gelman, D. L., and Maxfield, F. R. (1994). Quantification of low density lipoprotein and transferrin endocytic sorting HEp2 cells using confocal microscopy. J. Cell Sci. *107*(Pt 8), 2177–2189.

Hammes, A., *et al.* (2005). Role of endocytosis in cellular uptake of sex steroids. Cell *122*, 751–762.

Handley, D. A., Arbeeny, C. M., Witte, L. D., and Chien, S. (1981). Colloidal gold—low density lipoprotein conjugates as membrane receptor probes. Proc. Natl. Acad. Sci. USA *78*, 368–371.

Hanover, J. A., Willingham, M. C., and Pastan, I. (1984). Kinetics of transit of transferrin and epidermal growth factor through clathrin-coated membranes. Cell *39*, 283–293.

Hawryluk, M. J., Keyel, P. A., Mishra, S. K., Watkins, S. C., Heuser, J. E., and Traub, L. M. (2006). Epsin 1 is a polyubiquitin-selective clathrin-associated sorting protein. Traffic *7*, 262–281.

He, G., Gupta, S., Yi, M., Michaely, P., Hobbs, H. H., and Cohen, J. C. (2002). ARH is a modular adaptor protein that interacts with the LDL receptor, clathrin and AP-2. J. Biol. Chem. *277*, 44044–44049.

Heuser, J. (1980). Three-dimensional visualization of coated vesicle formation in fibroblasts. J. Cell Biol. *84*, 560–583.

Heuser, J. E. (2000). Membrane traffic in anaglyph stereo. Traffic *1*, 35–37.

Heuser, J. E., and Anderson, R.G.W. (1989). Hypertonic media inhibit receptor-mediated endocytosis by blocking clathrin-coated pit formation. J. Cell Biol. *108*, 389–400.

Hinrichsen, L., Harborth, J., Andrees, L., Weber, K., and Ungewickell, E. J. (2003). Effect of clathrin heavy chain- and α-adaptin specific small interfering RNAs on endocytic accessory proteins and receptor trafficking in HeLa cells. J. Biol. Chem. *278*, 45160–45170.

Hinrichsen, L., Meyerholz, A., Groos, S., and Ungewickell, E. J. (2006). Bending a membrane: How clathrin affects budding. Proc. Nat. Acad. Sci. USA *103*, 8715–8720.

Hocevar, B. A., Smine, A., Xu, X. X., and Howe, P. H. (2001). The adaptor molecule Disabled-2 links the transforming growth factor beta receptors to the Smad pathway. EMBO J. *20*, 2789–2801.

Höning, S., Ricotta, D., Krauss, M., Spate, K., Spolaore, B., Motley, A., Robinson, M., Robinson, C., Haucke, V., and Owen, D. J. (2005). Phosphatidylinositol-(4,5)-bisphosphate regulates sorting signal recognition by the clathrin-associated adaptor complex AP2. Mol. Cell *18*, 519–531.

Huang, F., Khvorova, A., Marshall, W., and Sorkin, A. (2004). Analysis of clathrin-mediated endocytosis of epidermal growth factor receptor by RNA interference. J. Biol. Chem. *279*, 16657–16661.

Hubbard, A. L., Wall, D. A., and Ma, A. (1983). Isolation of rat hepatocyte plasma membranes. I. Presence of the three major domains. J. Cell Biol. *96*, 217–229.

Jones, C., Hammer, R. E., Li, W. P., Cohen, J. C., Hobbs, H. H., and Herz, J. (2003). Normal sorting, but defective endocytosis of the LDL receptor in mice with autosomal recessive hypercholesterolemia. J. Biol. Chem. *278*, 29024–29030.

Keyel, P. A., Watkins, S. C., and Traub, L. M. (2004). Endocytic adaptor molecules reveal an endosomal population of clathrin by total internal reflection fluorescence microscopy. J. Biol. Chem. *279*, 13190–13204.

Kim, Y. M., and Benovic, J. L. (2002). Differential roles of arrestin-2 interaction with clathrin and adaptor protein 2 in G protein-coupled receptor trafficking. J. Biol. Chem. *277*, 30760–30768.

Lakadamyali, M., Rust, M. J., and Zhuang, X. (2006). Ligands for clathrin-mediated endocytosis are differentially sorted into distinct populations of early endosomes. Cell *124*, 997–1009.

Laporte, S. A., Oakley, R. H., Holt, J. A., Barak, L. S., and Caron, M. G. (2000). The interaction of β-arrestin with the AP-2 adaptor is required for the clustering of β_2-adrenergic receptor into clathrin-coated pits. J. Biol. Chem. *275*, 23120–23126.

Marks, M. S., Woodruff, L., Ohno, H., and Bonifacino, J. S. (1996). Protein targeting by tyrosine- and di-leucine-based signals: evidence for distinct saturable components. J. Cell Biol. *135*, 341–354.

Maurer, M. E., and Cooper, J. A. (2005). Endocytosis of megalin by visceral endoderm cells requires the Dab2 adaptor protein. J. Cell Sci. *118*, 5345–5355.

Maurer, M. E., and Cooper, J. A. (2006). The adaptor protein Dab2 sorts LDL receptors into coated pits independently of AP-2 and ARH. J. Cell Sci. (*in press*).

Maxfield, F. R., and McGraw, T. E. (2004). Endocytic recycling. Nat. Rev. Mol. Cell Biol. *5*, 121–132.

Merrifield, C. J., Feldman, M. E., Wan, L., and Almers, W. (2002). Imaging actin and dynamin recruitment during invagination of single clathrin-coated pits. Nat. Cell Biol. *4*, 691–698.

Merrifield, C. J., Perrais, D., and Zenisek, D. (2005). Coupling between clathrin-coated-pit invagination, cortactin recruitment, and membrane scission observed in live cells. Cell *121*, 593–606.

Minamide, L. S., and Bamburg, J. R. (1990). A filter paper dye-binding assay for quantitative determination of protein without interference from reducing agents or detergents. Anal. Biochem. *190*, 66–70.

Mishra, S. K., Keyel, P. A., Edeling, M. A., Owen, D. J., and Traub, L. M. (2005). Functional dissection of an AP-2 β2 appendage-binding sequence within the autosomal recessive hypercholesterolemia (ARH) protein. J. Biol. Chem. *280*, 19270–19280.

Mishra, S. K., Keyel, P. A., Hawryluk, M. J., Agostinelli, N. R., Watkins, S. C., and Traub, L. M. (2002a). Disabled-2 exhibits the properties of a cargo-selective endocytic clathrin adaptor. EMBO J. *21*, 4915–4926.

Mishra, S. K., Watkins, S. C., and Traub, L. M. (2002b). The autosomal recessive hypercholesterolemia (ARH) protein interfaces directly with the clathrin-coat machinery. Proc. Natl. Acad. Sci. USA *99*, 16099–16104.

Morris, S. M., and Cooper, J. A. (2001). Disabled-2 colocalizes with the LDLR in clathrin-coated pits and interacts with AP-2. Traffic *2*, 111–123.

Morris, S. M., Tallquist, M. D., Rock, C. O., and Cooper, J. A. (2002). Dual roles for the Dab2 adaptor protein in embryonic development and kidney transport. EMBO J. *21*, 1555–1564.

Motley, A., Bright, N. A., Seaman, M. N., and Robinson, M. S. (2003). Clathrin-mediated endocytosis in AP-2-depleted cells. J. Cell Biol. *162*, 909–918.

Naoumova, R. P., Neuwirth, C., Lee, P., Miller, J. P., Taylor, K. G., and Soutar, A. K. (2004). Autosomal recessive hypercholesterolaemia: long-term follow up and response to treatment. Atherosclerosis *174*, 165–172.

Nathke, I. S., Heuser, J., Lupas, A., Stock, J., Turck, C. W., and Brodsky, F. M. (1992). Folding and trimerization of clathrin subunits at the triskelion hub. Cell *68*, 899–910.

Neutra, M. R., Ciechanover, A., Owen, L. S., and Lodish, H. F. (1985). Intracellular transport of transferrin- and asialoorosomucoid-colloidal gold conjugates to lysosomes after receptor-mediated endocytosis. J. Histochem. Cytochem. *33*, 1134–1144.

Ohno, H., Stewart, J., Fournier, M.-C., Bosshart, H., Rhee, I., Miyatake, S., Saito, T., Galluser, A., Kirchhausen, T., and Bonifacino, J. S. (1995). Interaction of tyrosine-based sorting signals with clathrin-associated proteins. Science *269*, 1872–1875.

Olusanya, O., Andrews, P. D., Swedlow, J. R., and Smythe, E. (2001). Phosphorylation of threonine 156 of the μ2 subunit of the AP2 complex is essential for endocytosis in vitro and in vivo. Curr. Biol. *11*, 896–900.

Orci, L., Carpentier, J. L., Perrelet, A., Anderson, R. G., Goldstein, J. L., and Brown, M. S. (1978). Occurrence of low density lipoprotein receptors within large pits on the surface of human fibroblasts as demonstrated by freeze-etching. Exp. Cell Res. *113*, 1–13.

Osono, Y., Woollett, L. A., Herz, J., and Dietschy, J. M. (1995). Role of the low density lipoprotein receptor in the flux of cholesterol through the plasma and across the tissues of the mouse. J. Clin. Invest. *95*, 1124–1132.

Owen, D. J., Collins, B. M., and Evans, P. R. (2004). Adaptors for clathrin coats: structure and function. Annu. Rev. Cell Dev. Biol. *20*, 153–191.

Paavola, L. G., Strauss, J. F., 3rd, Boyd, C. O., and Nestler, J. E. (1985). Uptake of gold- and [^{3}H]cholesteryl linoleate-labeled human low density lipoprotein by cultured rat granulosa cells: cellular mechanisms involved in lipoprotein metabolism and their importance to steroidogenesis. J. Cell Biol. *100*, 1235–1247.

Panakova, D., Sprong, H., Marois, E., Thiele, C., and Eaton, S. (2005). Lipoprotein particles are required for Hedgehog and Wingless signalling. Nature *435*, 58–65.

Rappoport, J. Z., Taha, B. W., Lemeer, S., Benmerah, A., and Simon, S. M. (2003). The AP2 complex is excluded from the dynamic population of plasma membrane associated clathrin. J. Biol. Chem. 47357–47360.

Rink, J., Ghigo, E., Kalaidzidis, Y., and Zerial, M. (2005). Rab conversion as a mechanism of progression from early to late endosomes. Cell *122*, 735–749.

Robinson, M. S. (2004). Adaptable adaptors for coated vesicles. Trends Cell Biol. *14*, 167–174.

Roth, T. F., and Porter, K. R. (1964). Yolk protein uptake in the oocyte of the mosquito *Aedes aegypti*. L. J. Cell Biol. *20*, 313–332.

Sanan, D. A., and Anderson, R. G. (1991). Simultaneous visualization of LDL receptor distribution and clathrin lattices on membranes torn from the upper surface of cultured cells. J. Histochem. Cytochem. *39*, 1017–1024.

Sanan, D. A., Van der Westhuyzen, D. R., Gevers, W., and Coetzee, G. A. (1987). The surface distribution of low density lipoprotein receptors on cultured fibroblasts and endothelial cells. Ultrastructural evidence for dispersed receptors. Histochemistry *86*, 517–523.

Santini, F., Gaidarov, I., and Keen, J. H. (2002). G protein-coupled receptor/arrestin3 modulation of the endocytic machinery. J. Cell Biol. *156*, 665–676.

Santini, F., Marks, M. S., and Keen, J. H. (1998). Endocytic clathrin-coated pit formation is independent of receptor internalization signal levels. Mol. Biol. Cell *9*, 1177–1194.

Schmid, E. M., Ford, M. G., Burtey, A., Praefcke, G. J., Peak Chew, S. Y., Mills, I. G., Benmerah, A., and Mcmahon, H. T. (2006). Role of the AP2 β-appendage hub in recruiting partners for clathrin coated vesicle assembly. PLoS Biol. *4* (*in press*).

Scott, M. G., Benmerah, A., Muntaner, O., and Marullo, S. (2002). Recruitment of activated G protein-coupled receptors to pre-existing clathrin-coated pits in living cells. J. Biol. Chem. *277*, 3552–3559.

Sorkin, A. (2004). Cargo recognition during clathrin-mediated endocytosis: a team effort. Curr. Opin. Cell Biol. *16*, 392–399.

Stolt, P. C., Vardar, D., and Blacklow, S. C. (2004). The dual-function disabled-1 PTB domain exhibits site independence in binding phosphoinositide and peptide ligands. Biochemistry *43*, 10979–10987.

Stoorvogel, W., Geuze, H. J., and Strous, G. J. (1987). Sorting of endocytosed transferrin and asialoglycoprotein occurs immediately after internalization in HepG2 cells. J. Cell Biol. *104*, 1261–1268.

Tabas, I., and Kornfeld, S. (1979). Purification and characterization of a rat liver Golgi alpha-mannosidase capable of processing asparagine-linked oligosaccharides. J. Biol. Chem. *254*, 11655–11663.

Tebar, F., Sorkina, T., Sorkin, A., Ericsson, M., and Kirchhausen, T. (1996). eps15 is a component of clathrin-coated pits and vesicles and is located at the rim of clathrin-coated pits. J. Biol. Chem. *271*, 28727–28730.

Toshima, J. Y., Toshima, J., Kaksonen, M., Martin, A. C., King, D. S., and Drubin, D. G. (2006). Spatial dynamics of receptor-mediated endocytic trafficking in budding yeast revealed by using fluorescent α-factor derivatives. Proc. Natl. Acad. Sci. USA *103*, 5793–5798.

Tosoni, D., Puri, C., Confalonieri, S., Salcini, A. E., De Camilli, P., Tacchetti, C., and Di Fiore, P. P. (2005). TTP specifically regulates the internalization of the transferrin receptor. Cell *123*, 875–888.

Traub, L. M. (2003). Sorting it out: AP-2 and alternate clathrin adaptors in endocytic cargo selection. J. Cell Biol. *163*, 203–208.

Traub, L. M., Bannykh, S. I., Rodel, J. E., Aridor, M., Balch, W. E., and Kornfeld, S. (1996). AP-2–containing clathrin coats assemble on mature lysosomes. J. Cell Biol. *135*, 1801–1804.

Traub, L. M., Kornfeld, S., and Ungewickell, E. (1995). Different domains of the AP-1 adaptor complex are required for Golgi membrane binding and clathrin recruitment. J. Biol. Chem. *270*, 4933–4942.

Via, D. P., Willingham, M. C., Pastan, I., Gotto, A. M., Jr., and Smith, L. C. (1982). Co-clustering and internalization of low-density lipoproteins and α_2-macroglobulin in human skin fibroblasts. Exp. Cell Res. *141*, 15–22.

Wang, H., *et al.* (2006). Clathrin-mediated endocytosis of ENaC: role of epsin. J. Biol. Chem. *281*, 14129–14135.

Warren, R. A., Green, F. A., Stenberg, P. E., and Enns, C. A. (1998). Distinct saturable pathways for the endocytosis of different tyrosine motifs. J. Biol. Chem. *273*, 17056–17063.

Willingham, M. C., Haigler, H. T., Fitzgerald, D. J., Gallo, M. G., Rutherford, A. V., and Pastan, I. H. (1983). The morphologic pathway of binding and internalization of epidermal growth factor in cultured cells. Studies on A431, KB, and 3T3 cells, using multiple methods of labelling. Exp. Cell Res. *146*, 163–175.

Willingham, M. C., Pastan, I. H., Sahagian, G. G., Jourdian, G. W., and Neufeld, E. F. (1981). Morphologic study of the internalization of a lysosomal enzyme by the mannose 6-phosphate receptor in cultured Chinese hamster ovary cells. Proc. Natl. Acad. Sci. USA *78*, 6967–6971.

Wollenberg, G. K., Semple, E., Quinn, B. A., and Hayes, M. A. (1987). Inhibition of proliferation of normal, preneoplastic, and neoplastic rat hepatocytes by transforming growth factor-β. Cancer Res. *47*, 6595–6599.

Wu, X., Zhao, X., Baylor, L., Kaushal, S., Eisenberg, E., and Greene, L. E. (2001). Clathrin exchange during clathrin-mediated endocytosis. J. Cell Biol. *155*, 291–300.

Wu, X., Zhao, X., Puertollano, R., Bonifacino, J. S., Eisenberg, E., and Greene, L. E. (2003). Adaptor and clathrin exchange at the plasma membrane and trans-Golgi network. Mol. Biol. Cell *14*, 516–528.

Xu, X. X., Yang, W., Jackowski, S., and Rock, C. O. (1995). Cloning of a novel phosphoprotein regulated by colony-stimulating factor 1 shares a domain with the *Drosophila disabled* gene product. J. Biol. Chem. *270*, 14184–14191.

Yim, Y. I., Scarselletta, S., Zang, F., Wu, X., Lee, D. W., Kang, Y. S., Eisenberg, E., and Greene, L. E. (2005). Exchange of clathrin, AP2 and epsin on clathrin-coated pits in permeabilized tissue culture cells. J. Cell Sci. *118*, 2405–2413.

Yun, M., Keshvara, L., Park, C. G., Zhang, Y. M., Dickerson, J. B., Zheng, J., Rock, C. O., Curran, T., and Park, H. W. (2003). Crystal structures of the dab homology domains of mouse disabled 1 and 2. J. Biol. Chem. *278*, 36572–36581.

Zuliani, G., *et al.* (1999). Characterization of a new form of inherited hypercholesterolemia: familial recessive hypercholesterolemia. Arterioscler. Thromb. Vasc. Biol. *19*, 802–809.